

# Non-Maxwellian analysis of *IRIS* TR lines

Jaroslav Dudík, Vanessa Polito,  
Elena Dzifčáková, Giulio Del Zanna, and Paola Testa



**Astronomical  
Institute**  
of the Czech Academy  
of Sciences

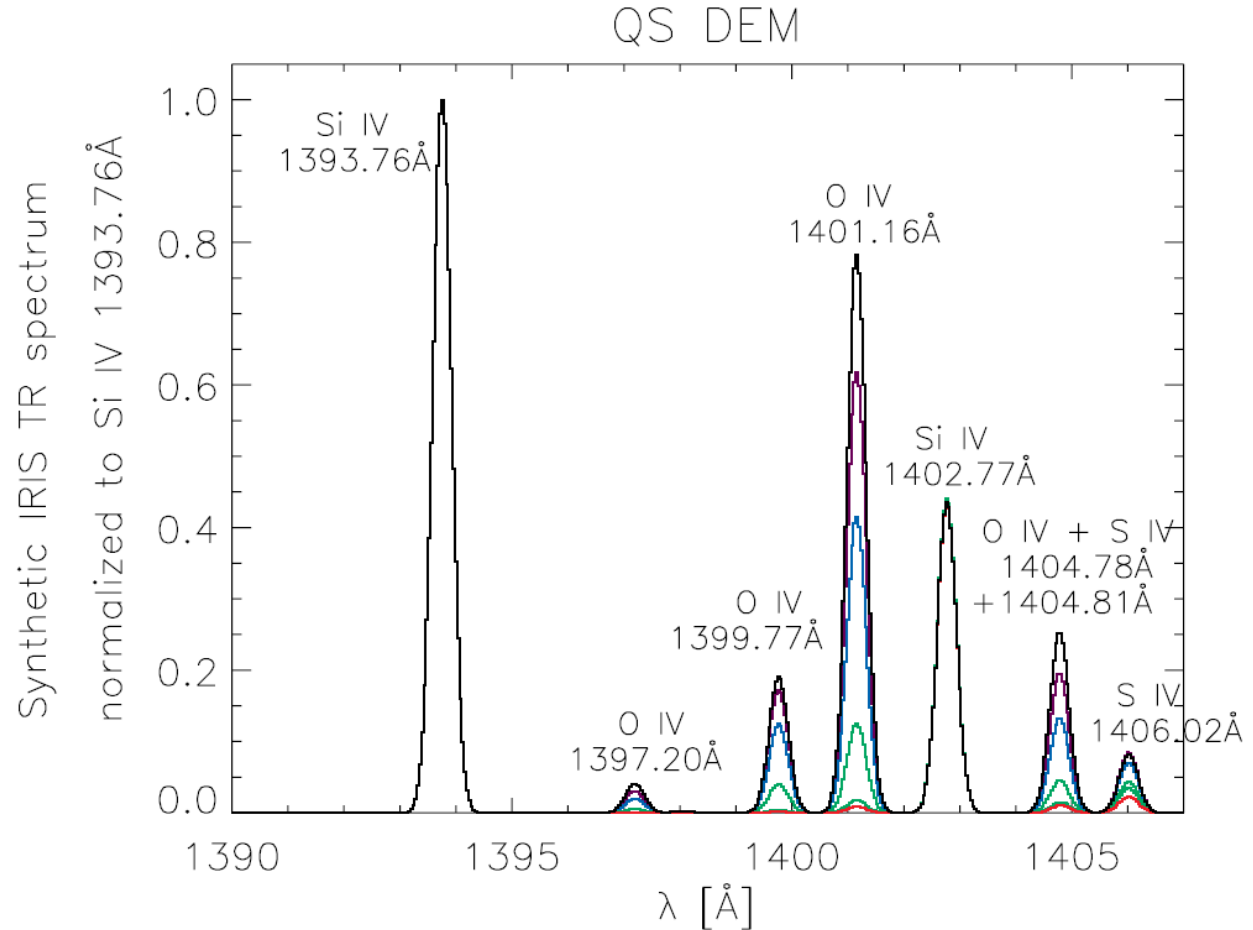
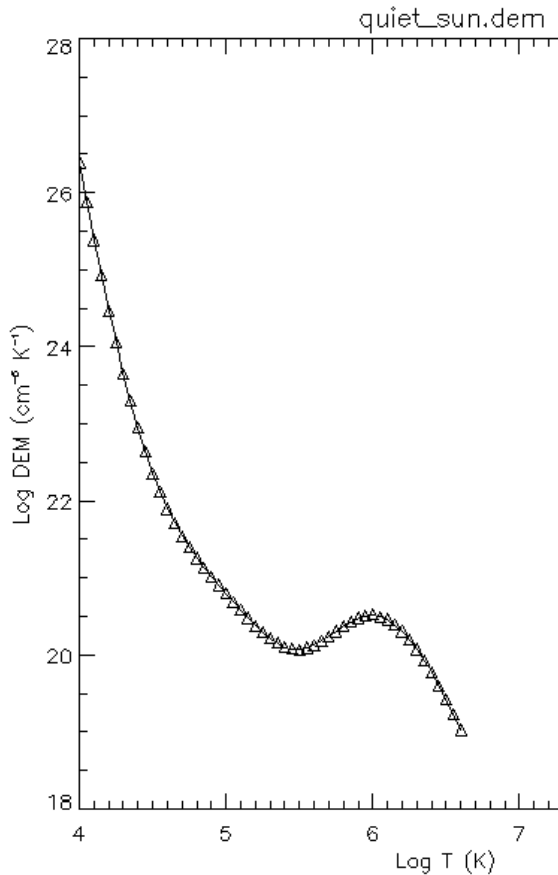


**UNIVERSITY OF  
CAMBRIDGE**



**Coronal Loops Workshop 8, Palermo  
2017 June 30**

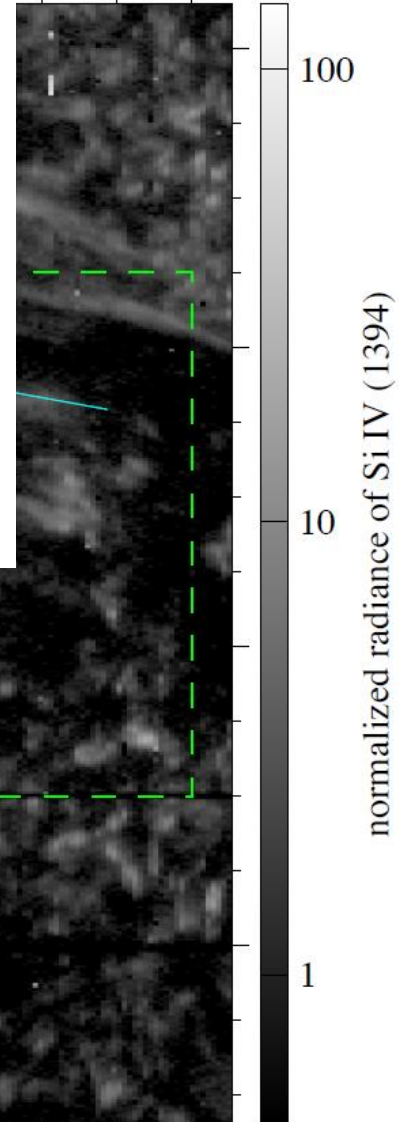
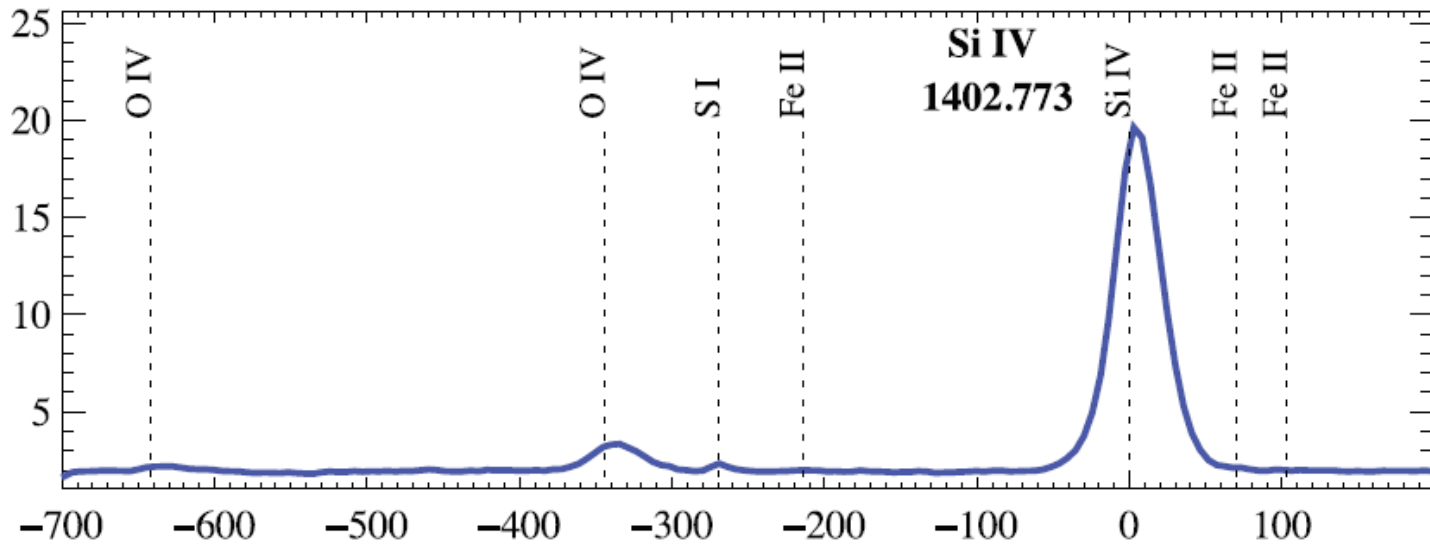
# Synthetic *IRIS* TR spectrum



*Dudík et al. (2014), ApJ 780, L12*

- Predicted *IRIS* FUV2 spectrum for a typical quiet Sun DEM:  
**O IV 1401.2 Å line stronger than the Si IV 1402.8 Å**
- For AR, with steeper DEM slope, O IV > Si IV also

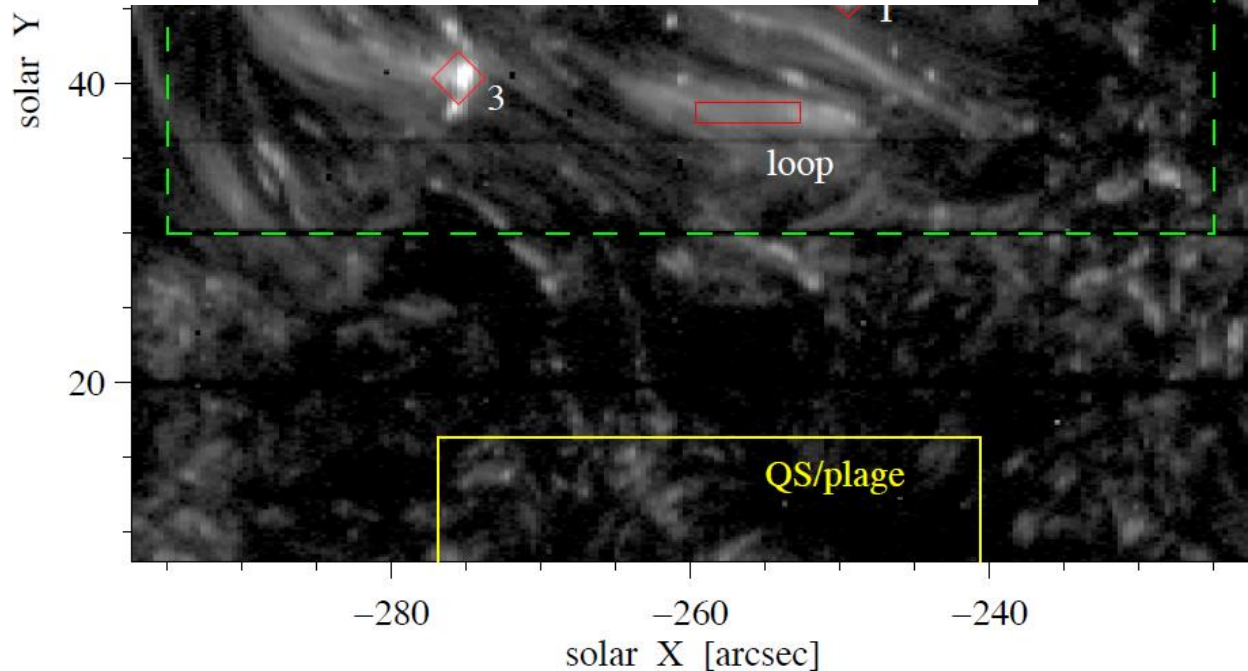
# TR Lines: Challenges



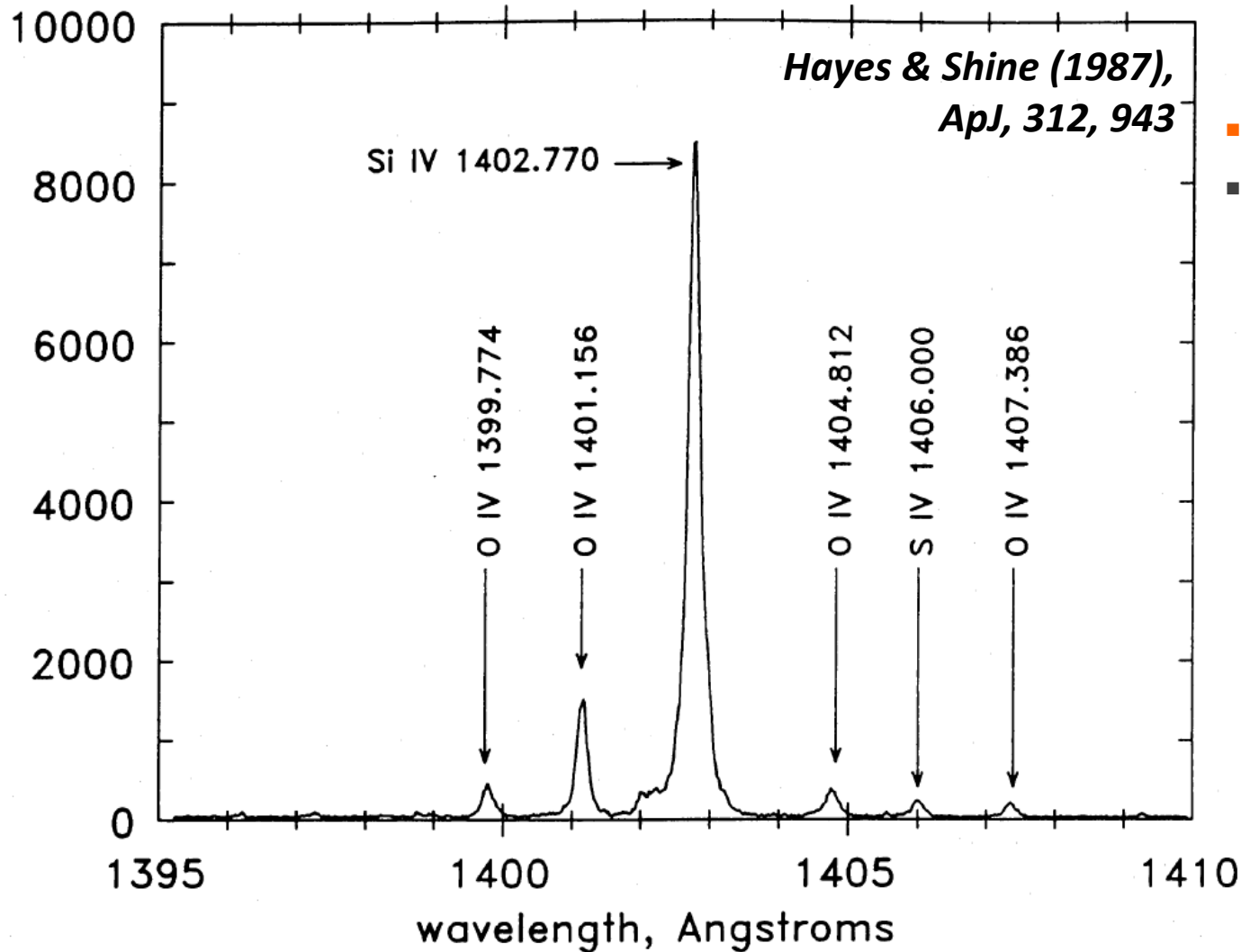
QS/Plage average spectrum (*IRIS*):

O IV lines very weak

*Peter et al. (2014)*  
*Sci 346, 1255726*



# TR Lines: Challenges



- Typical TR spectrum
- Seen with many instruments (*SMM/UVSP*, *SOHO/SUMER*, *IRIS*)

*Doyle & Raymond (1984)*

*Judge et al. (1995)*

*Curdt et al. (2001)*

*Doschek & Mariska (2001)*

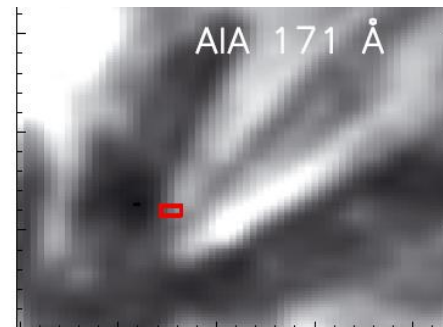
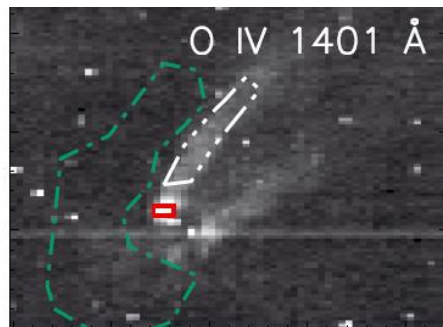
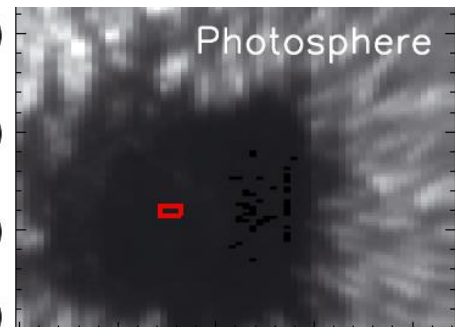
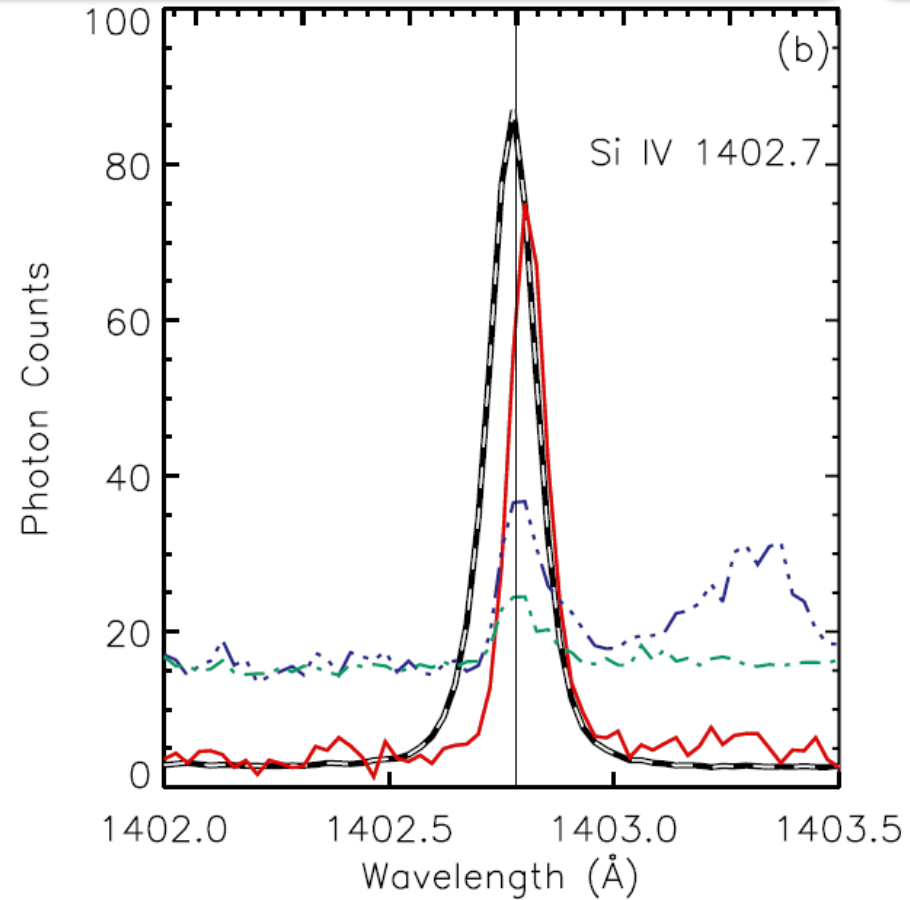
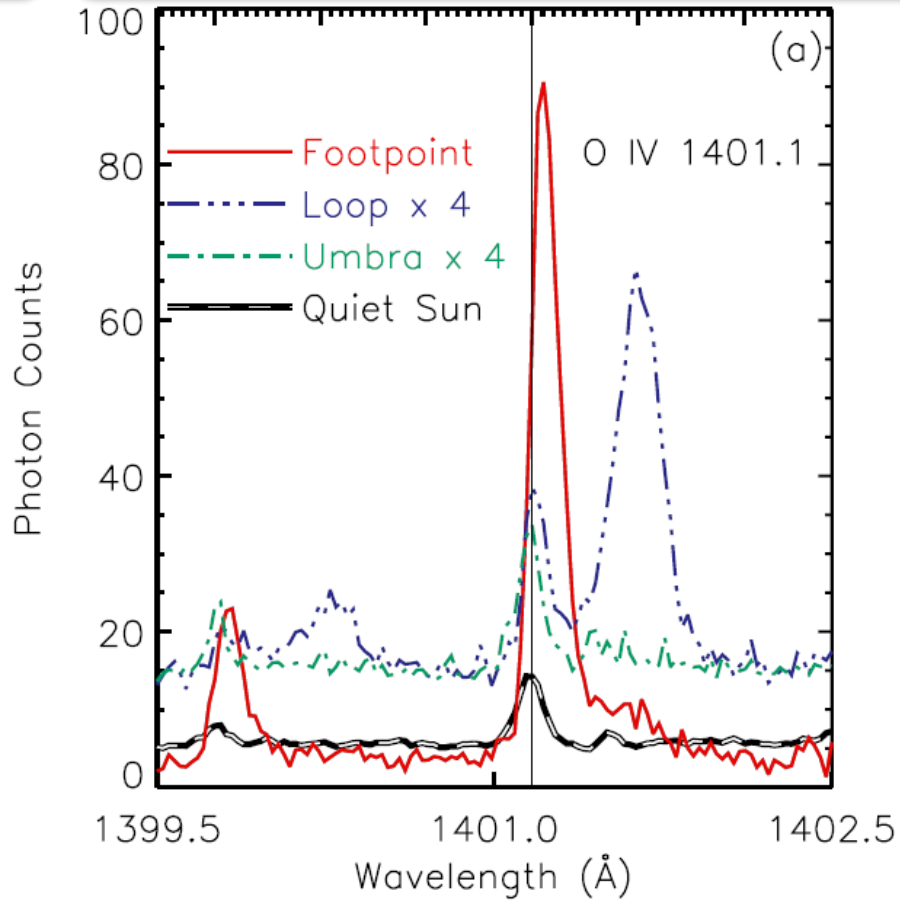
*Del Zanna et al. (2002)*

*Peter et al. (2014)*

*Polito et al. (2016)*

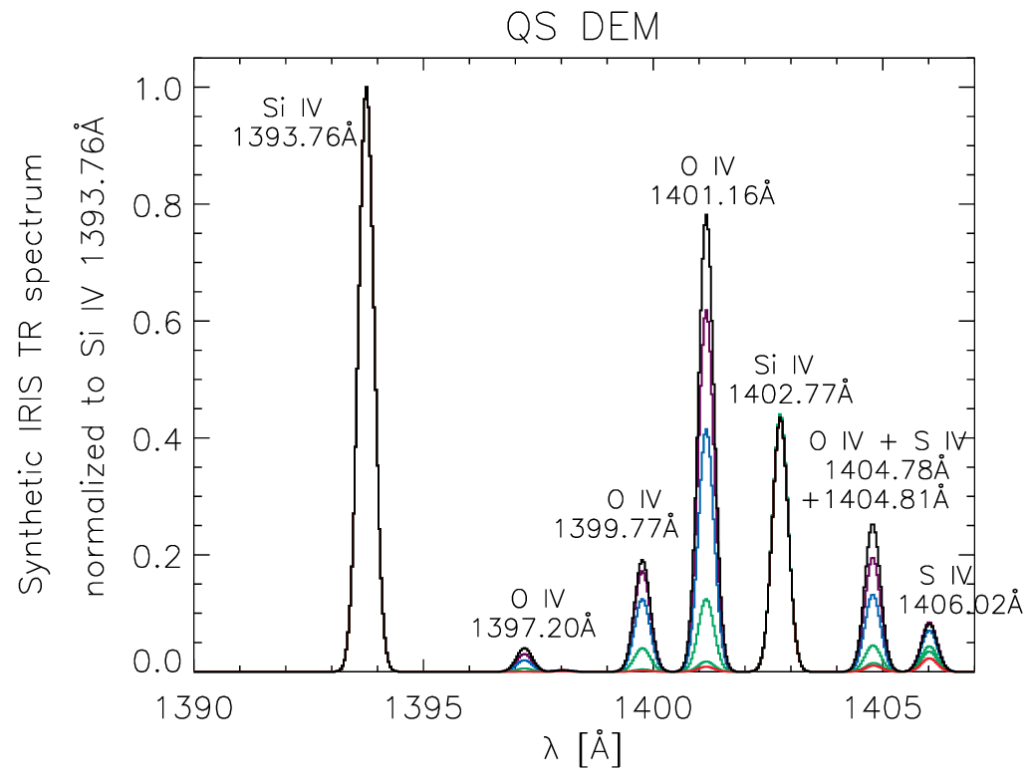
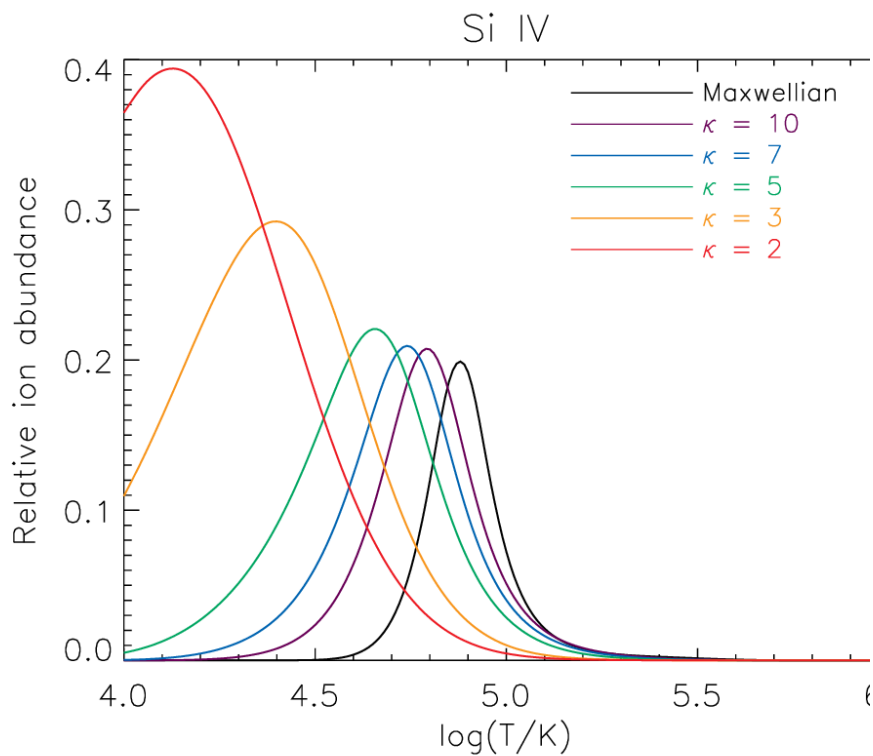
*Doschek et al. (2016)*

# O IV > Si IV ? : Single Solar Case



*Chitta et al. (2016),  
A&A, 587, A20*

# The $\kappa$ -distributions and TR lines



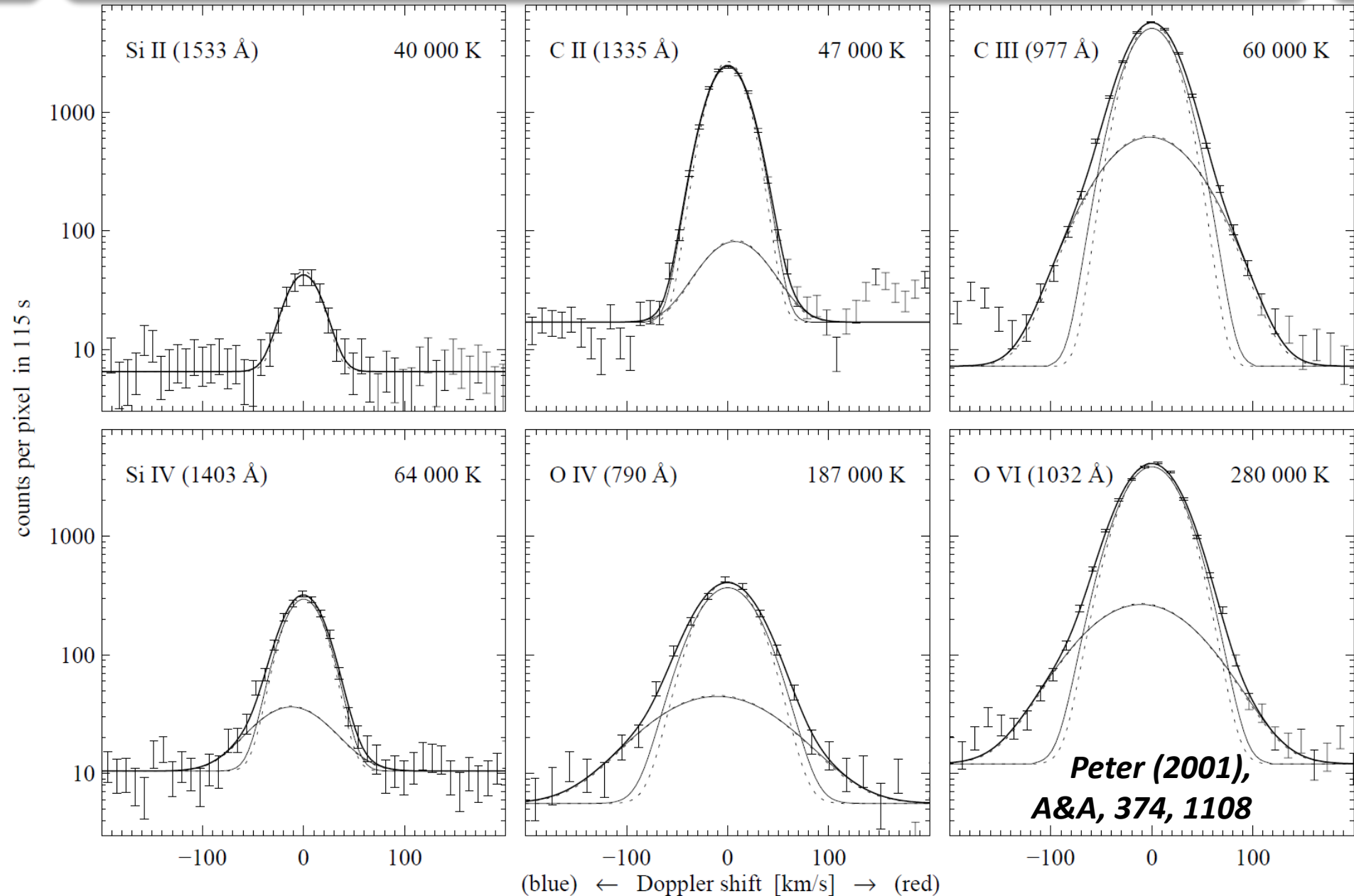
*Dzifčáková & Dudík (2013), ApJS, 206, 6*

*Dudík et al. (2014), ApJL, 780, L12*

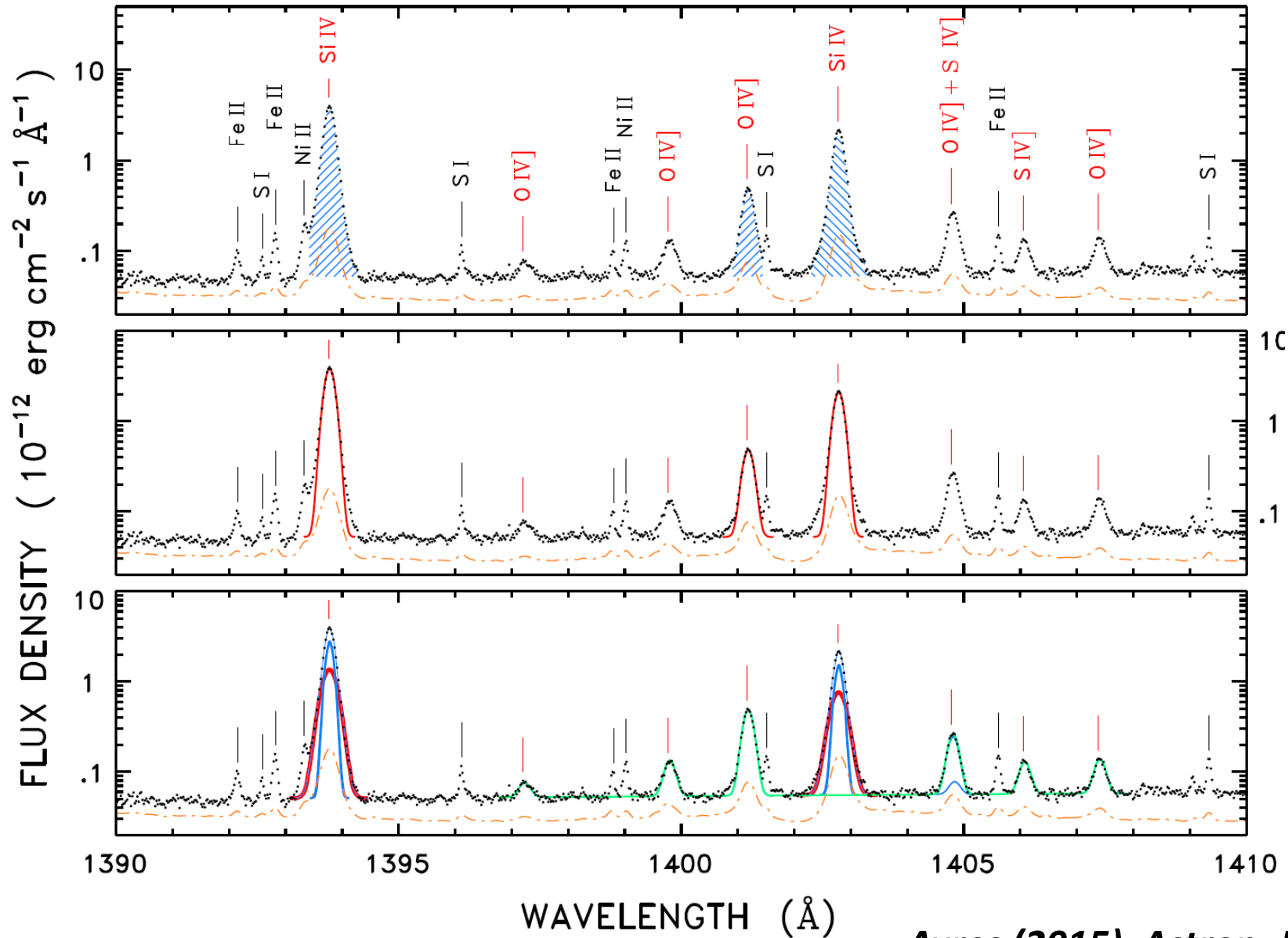
*Dzifčáková et al. (2017), A&A, in press*

- For TR lines, ion abundance peaks are shifted to lower  $T$
- High-energy tail: ionization rate enhanced by orders of magnitude
- Recombination enhanced by a factor of  $< 2$

# Non-Gaussian Line Profiles

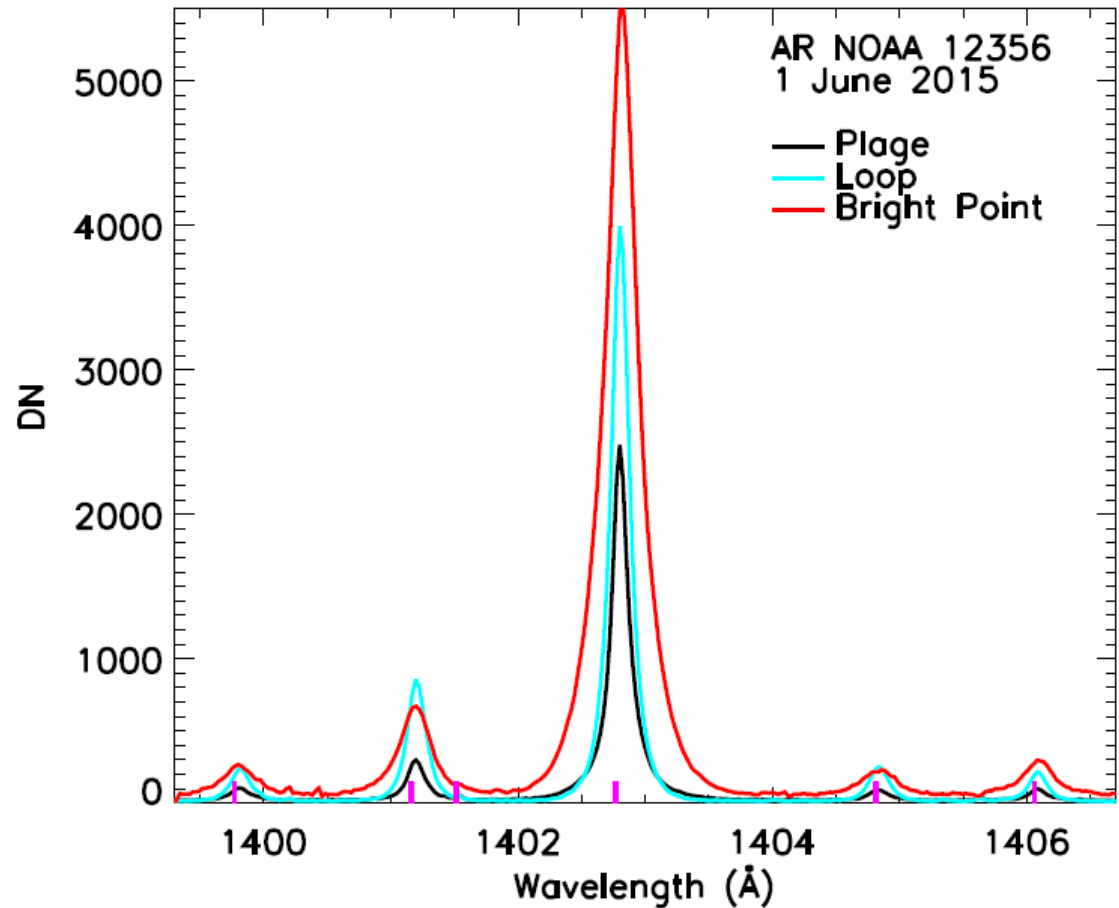
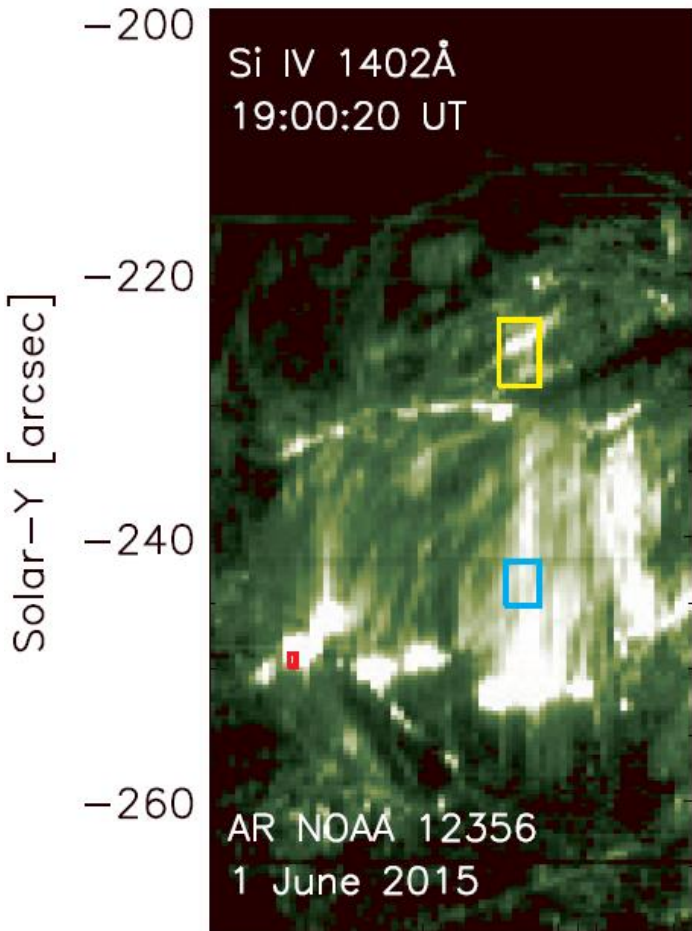


# $\alpha$ Centauri A+B





# Non-Gaussian Line Profiles: *IRIS*

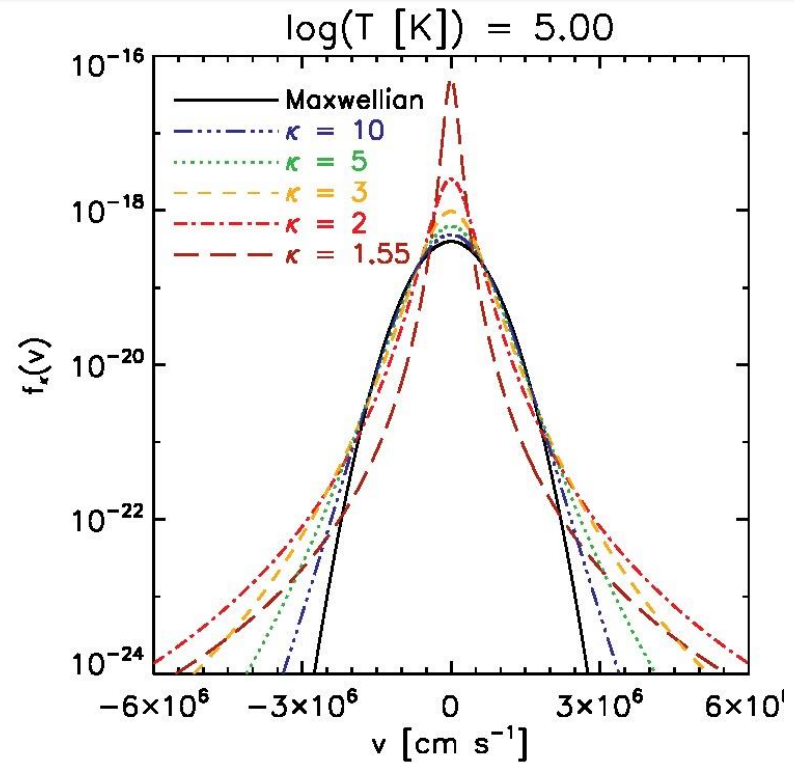
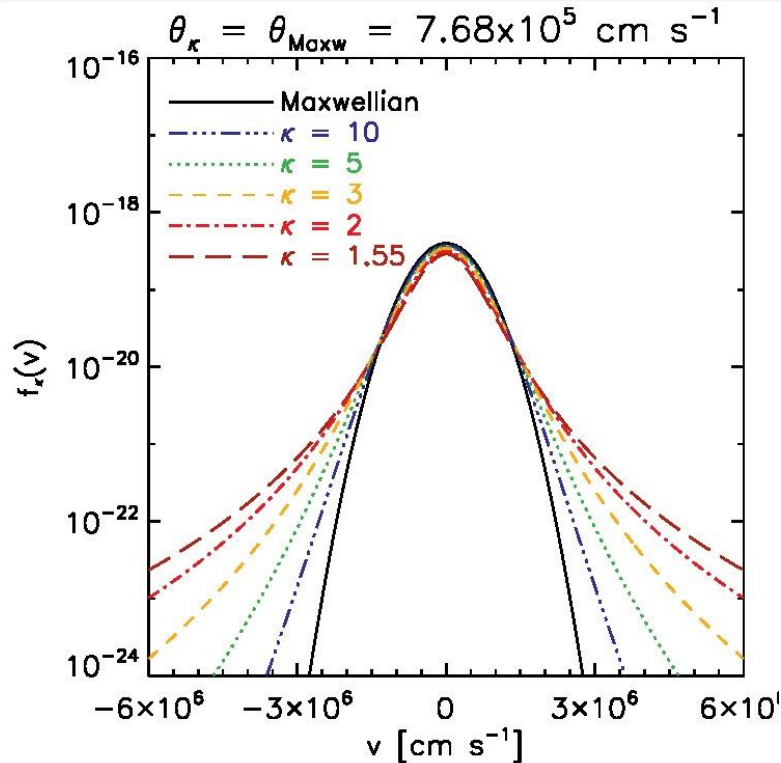


-90 -80 -70  
Solar-X [arcsec]

-90 -80  
Solar-X [arcsec]

-7 **Polito, Del Zanna, Dudík, et al.**  
**(2016), A&A, 594, A64**

# The $\kappa$ -distributions



$$f_\kappa(v)dv = \frac{C_\kappa}{(\pi(\kappa - 3/2)\theta^2)^{3/2}} \frac{dv}{\left(1 + \frac{v^2}{(\kappa - 3/2)\theta^2}\right)^{\kappa+1}}$$

$$T = \frac{m}{k_B} \int v^2 f_\kappa(v) d^3\vec{v} = \frac{m}{2k_B} \frac{2\kappa}{2\kappa - 3} \theta_\kappa^2$$

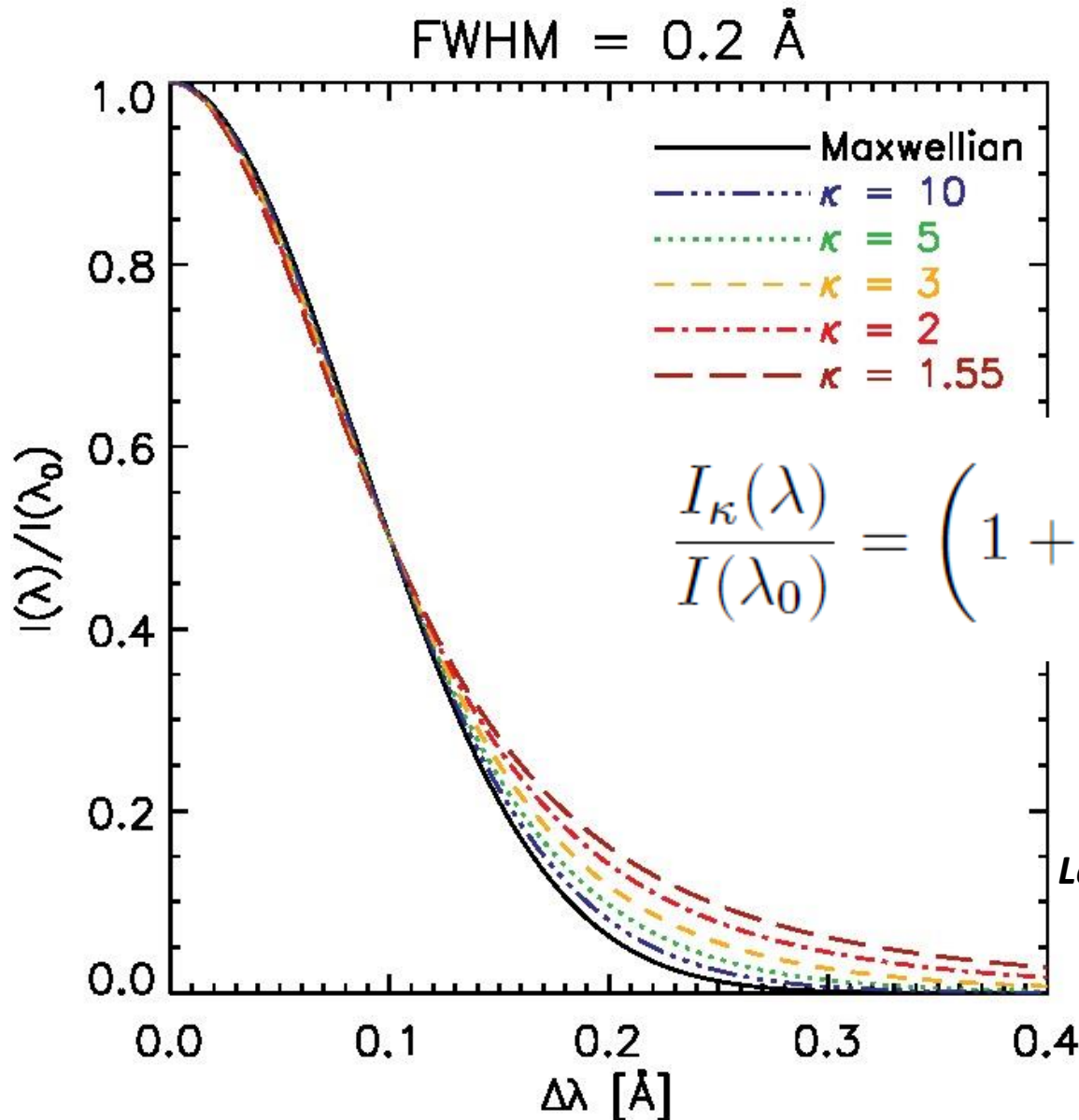
**Olbert (1968)**

**Vasilyunas (1968)**

**Livadiotis (2015)**

**Lazar et al. (2016)**

# $\kappa$ -Distributions and Line Profiles



$$\Delta\lambda/\lambda_0 = v_{\parallel}/c$$

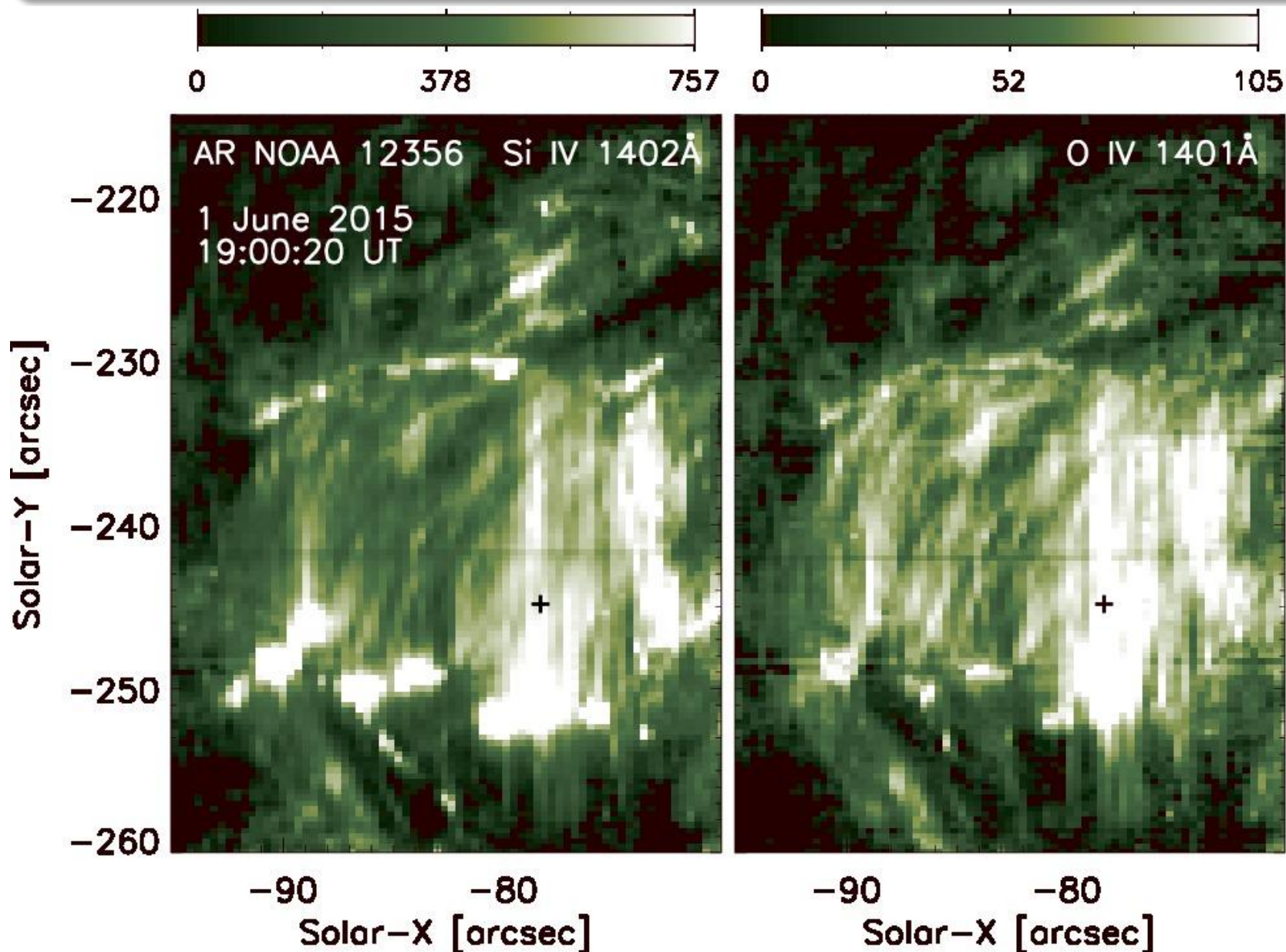


$$\frac{I_{\kappa}(\lambda)}{I(\lambda_0)} = \left( 1 + \frac{mc^2(\lambda - \lambda_0)^2}{2k_{\text{B}}T(\kappa - 3/2)\lambda_0^2} \right)^{-\kappa}$$

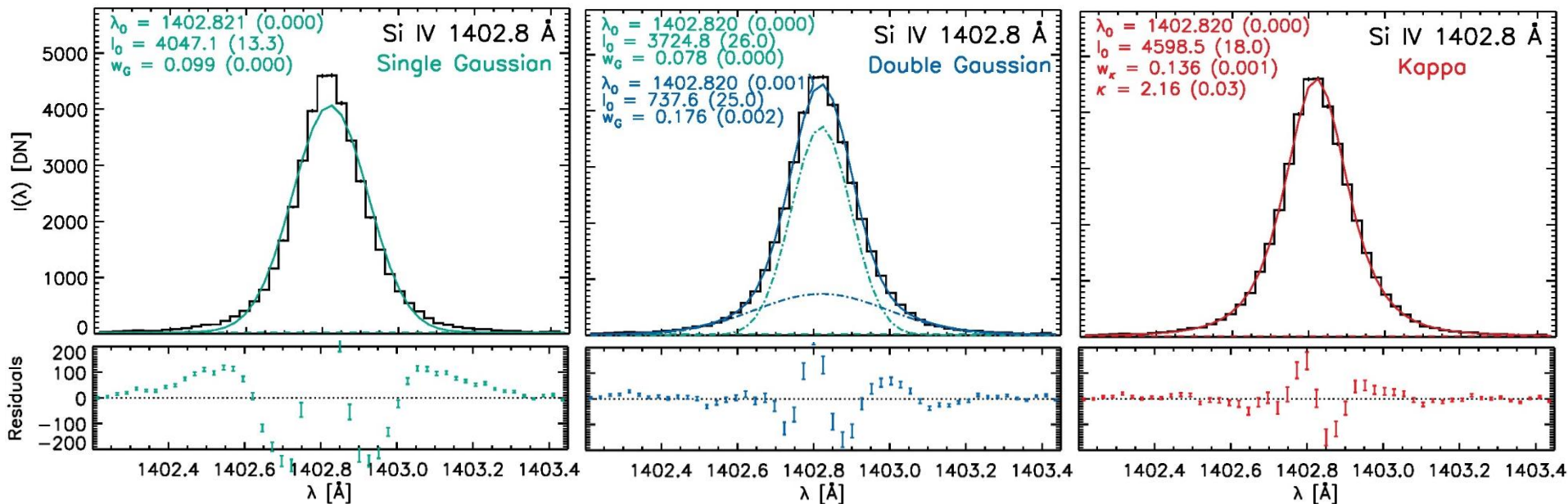
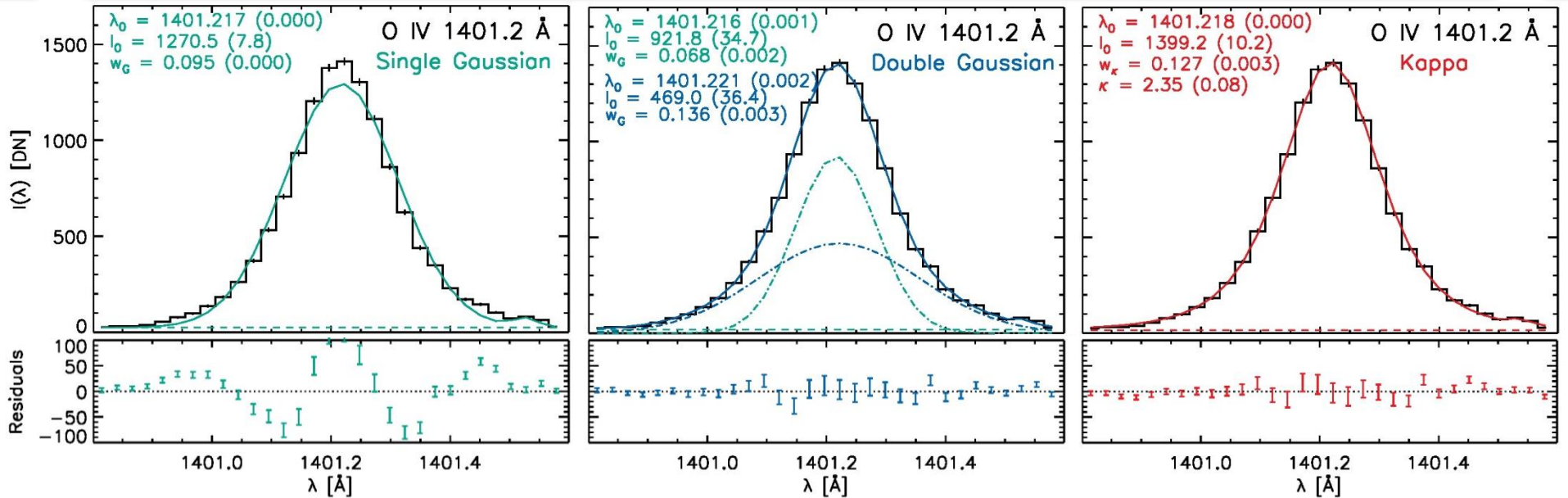
*Dzifčáková (1998), PhD Thesis*  
*Lee, Williams & Lapenta (2013), unpubl.*  
*Jeffrey et al. (2016), A&A, 590, A99*  
*Jeffrey et al. (2017), ApJ, 836, 35*

*Dudík et al. (2017), ApJ, 842, 19*

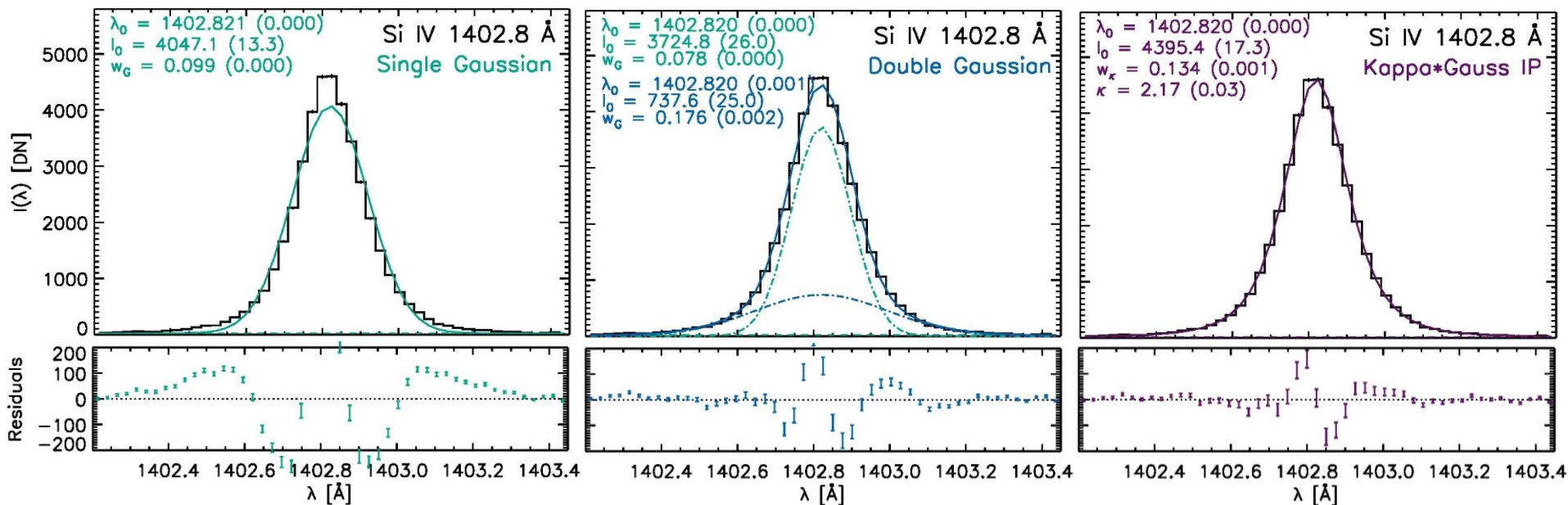
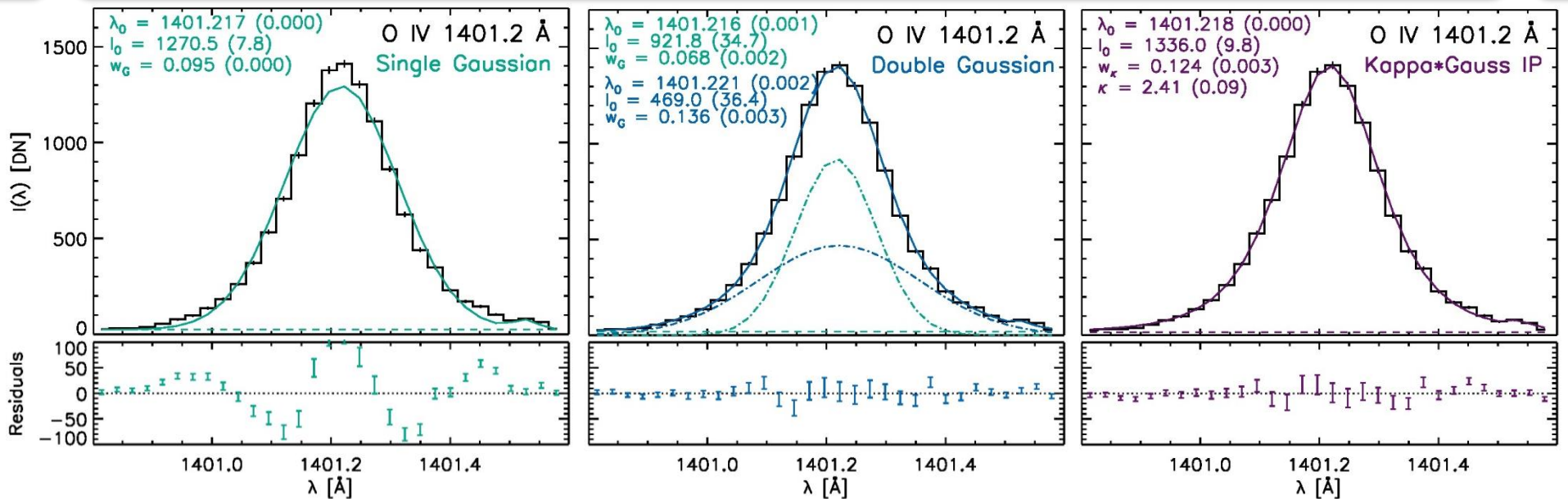
# IRIS Example Spectrum



# IRIS Example Spectrum: Fitting



# IRIS Example Spectrum: Fitting



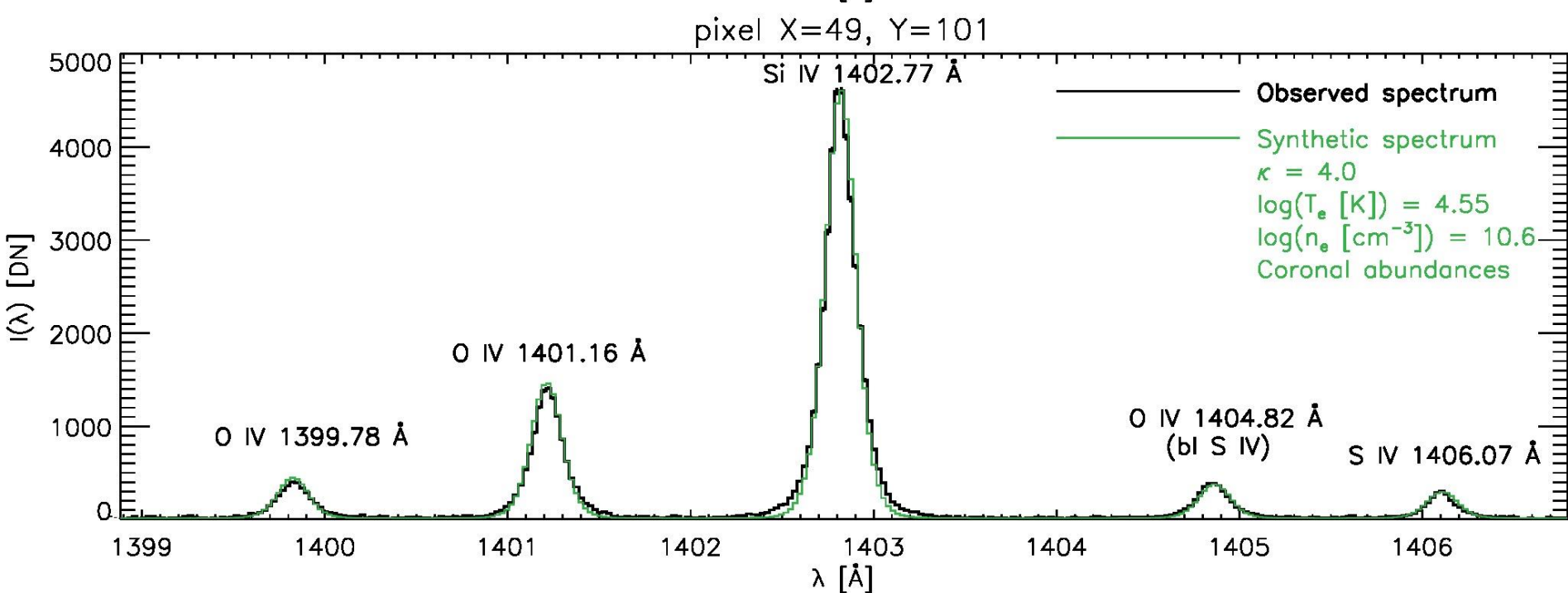
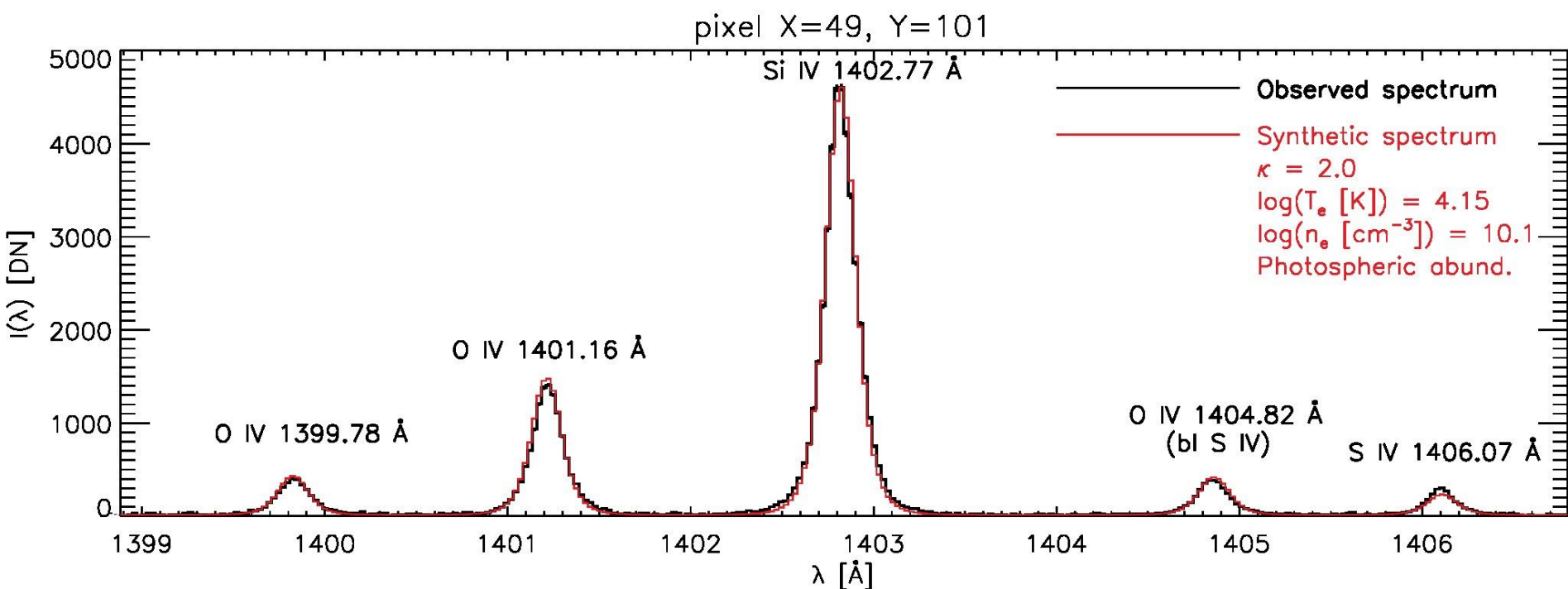
# IRIS Example Spectrum: Fitting

Line	$\lambda_0$ [Å]	$I_0$ [DN]	$w_\kappa$ [Å]	$\kappa$	FWHM $_\kappa$ [Å]	$T_i$ [MK]
O IV 1399.78 Å	1399.831 ± 0.001	385 ± 6	0.143 ± 0.010	2.16 ± 0.17	0.20 ± 0.08	1.81 ± 0.26
O IV 1401.16 Å	1401.218 ± 0.000	1399 ± 10	0.127 ± 0.003	2.35 ± 0.08	0.20 ± 0.05	1.43 ± 0.06
Si IV 1402.77 Å	1402.820 ± 0.000	4598 ± 18	0.136 ± 0.001	2.16 ± 0.03	0.19 ± 0.02	2.86 ± 0.06
O IV 1404.82 Å (bl S IV)	1404.855 ± 0.001	383 ± 6	0.163 ± 0.018	1.90 ± 0.13	0.19 ± 0.13	2.35 ± 0.52
S IV 1406.06 Å	1406.103 ± 0.001	282 ± 5	0.144 ± 0.021	1.91 ± 0.18	0.17 ± 0.17	3.64 ± 1.08

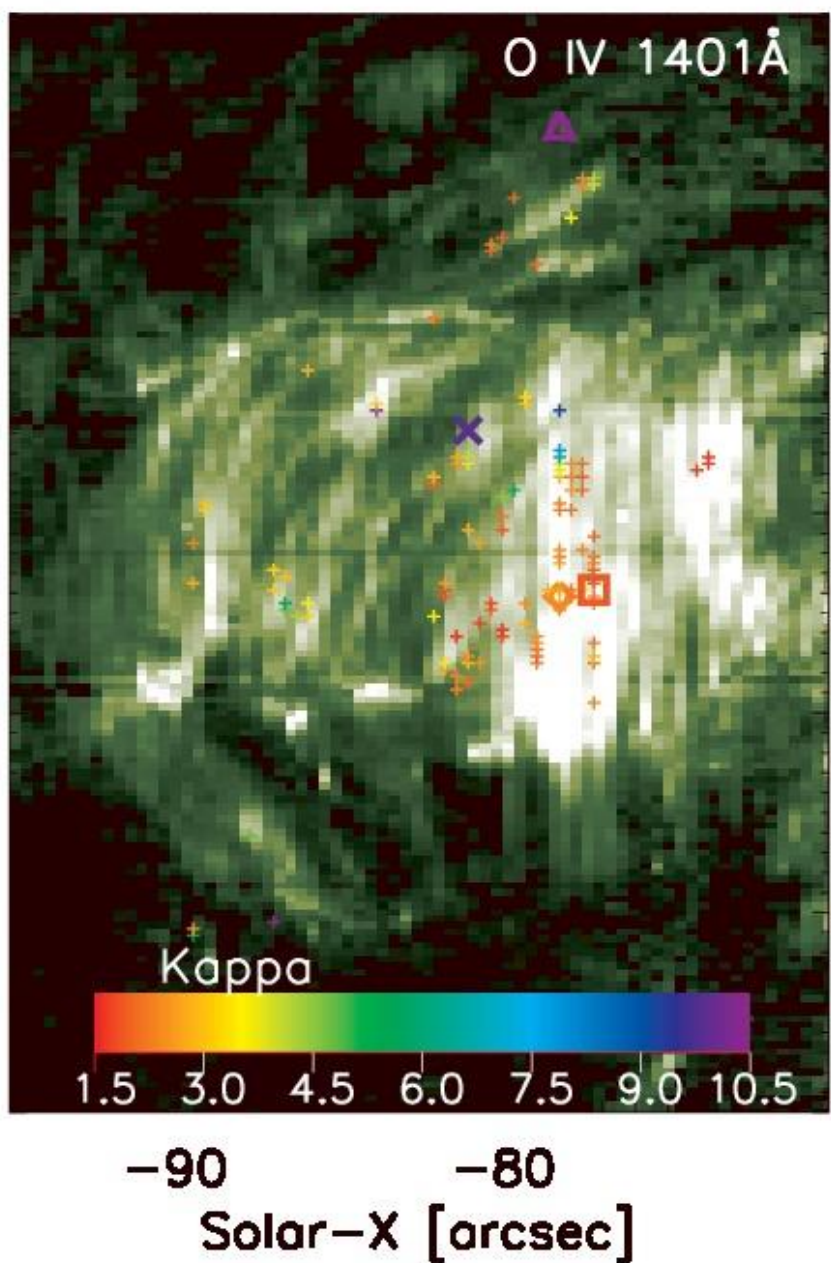
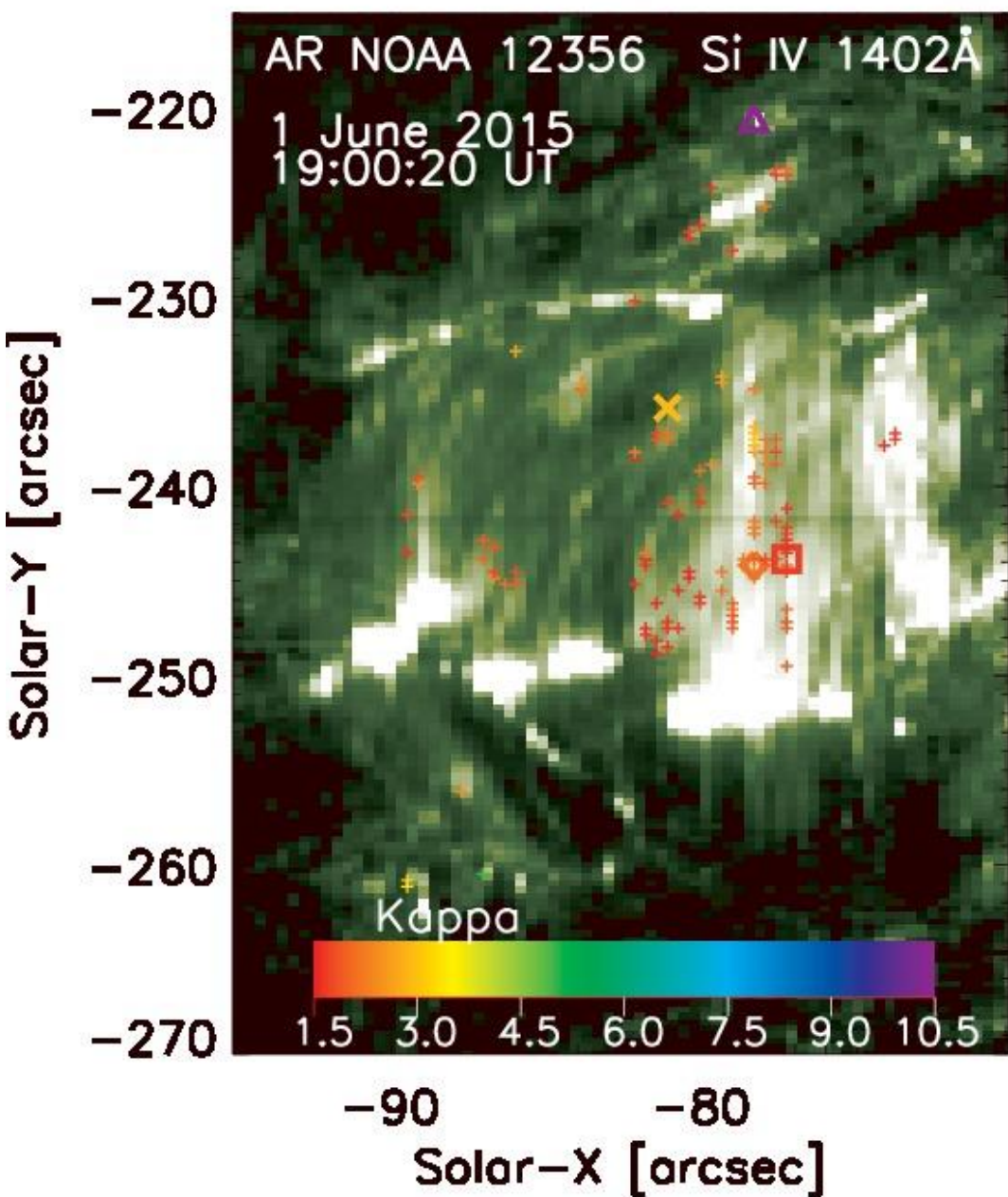
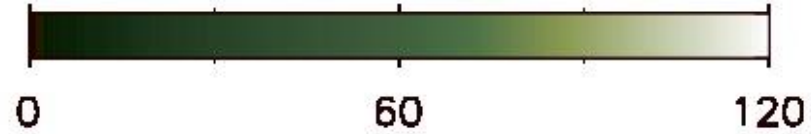
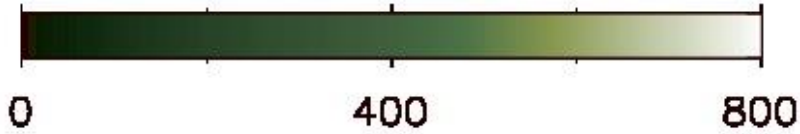
- (Almost) consistent  $\kappa$  values derived from all five TR lines
- All five lines have the same FWHM
- Significant non-thermal widths

$$w_\kappa^2 = \frac{1}{2} \frac{\lambda_0^2}{c^2} (\theta^2 + (\theta^{(\text{nth})})^2) = (w_\kappa^{(\text{th})})^2 + (w_\kappa^{(\text{nth})})^2$$

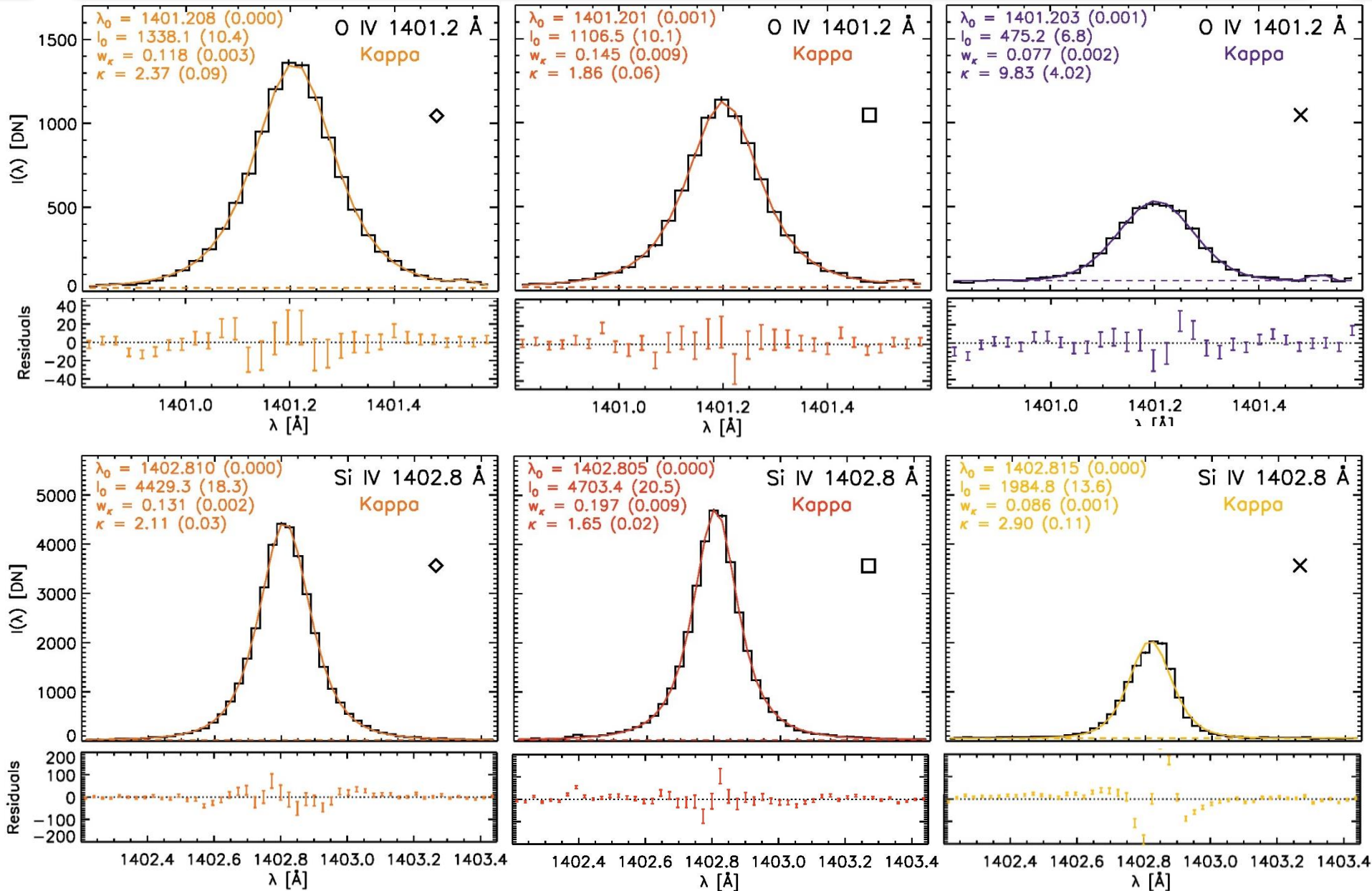
Line	$w_\kappa$ [Å]	$\log(T_{\text{max,Maxw}}$ [K])	$w_{\text{Maxw}}^{(\text{th})}$	$w_{\text{Maxw}}^{(\text{nth})}$	$\log(T_{\text{max},\kappa=2}$ [K])	$w_{\kappa=2}^{(\text{th})}$	$w_{\kappa=2}^{(\text{nth})}$
O IV 1399.78 Å	0.143 ± 0.010	5.15	0.040	0.137	4.45	0.018	0.141
O IV 1401.16 Å	0.127 ± 0.003	5.15	0.040	0.121	4.45	0.018	0.126
Si IV 1402.77 Å	0.136 ± 0.001	4.90	0.023	0.134	4.10	0.009	0.136
O IV 1404.82 Å (bl S IV)	0.163 ± 0.018	5.15	0.040	0.158	4.45	0.018	0.162
S IV 1406.06 Å	0.144 ± 0.021	5.05	0.025	0.141	4.20	0.009	0.143



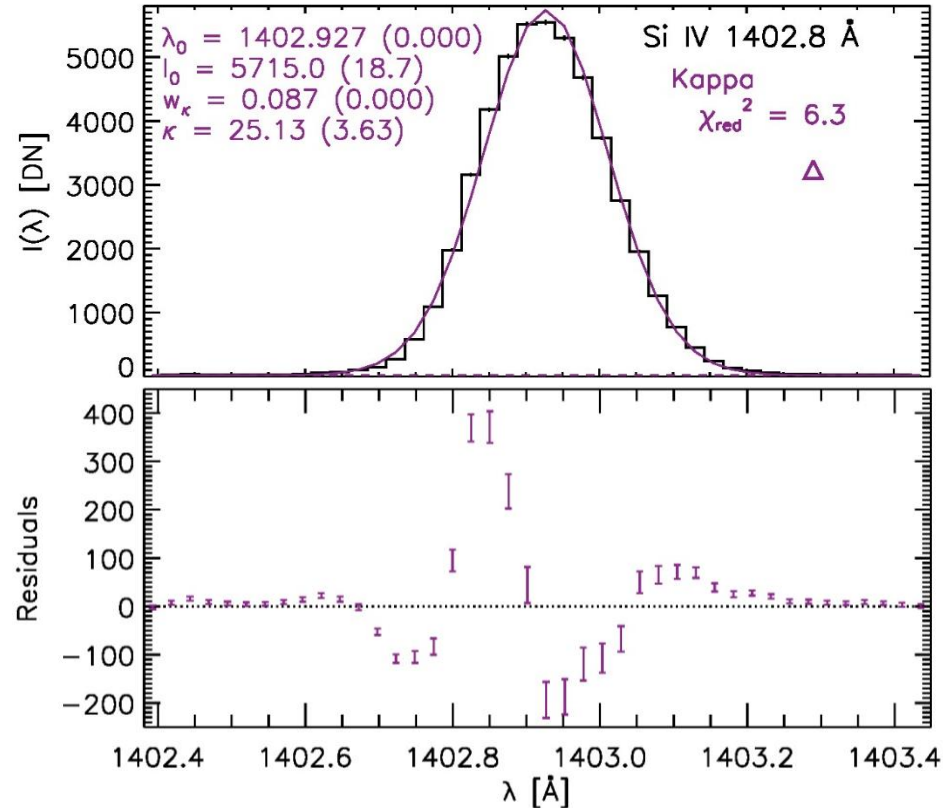
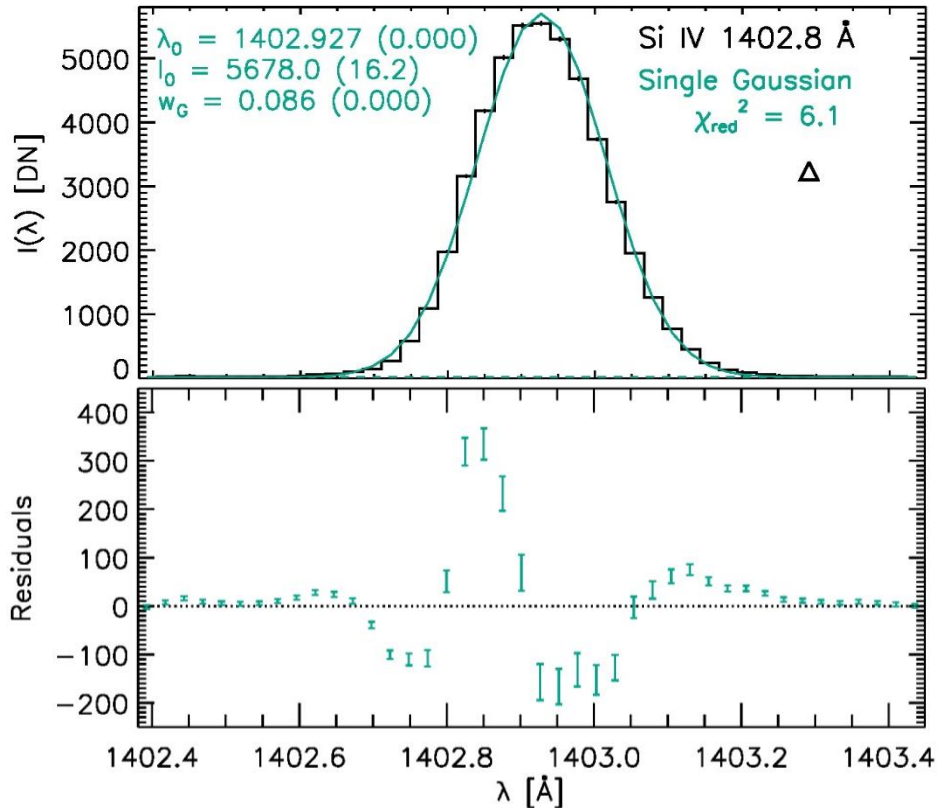




# More cases...



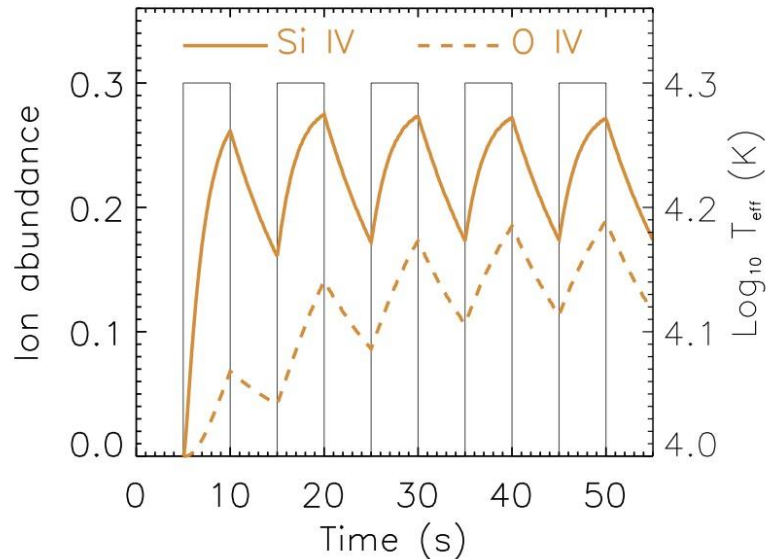
# Si IV: Case of a Gaussian Profile



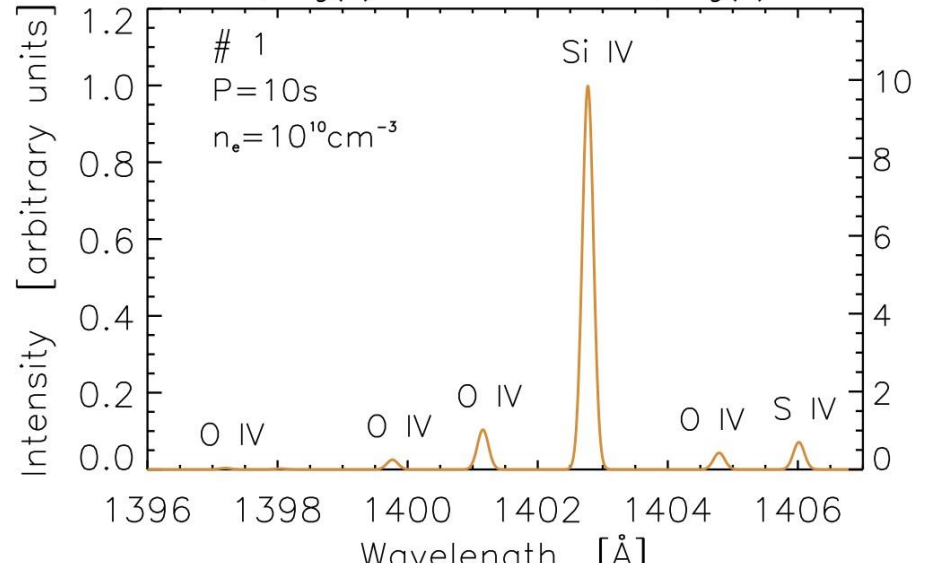
- Detection of a single, very bright Gaussian pixel
- Third brightest pixel with symmetric profiles
- The non-Gaussian profiles are *not* caused by instrumental effects
- Larger / asymmetric residuals: Possibly 2 Gaussian components

# Tails too strong? : $\kappa + \text{NEI}$

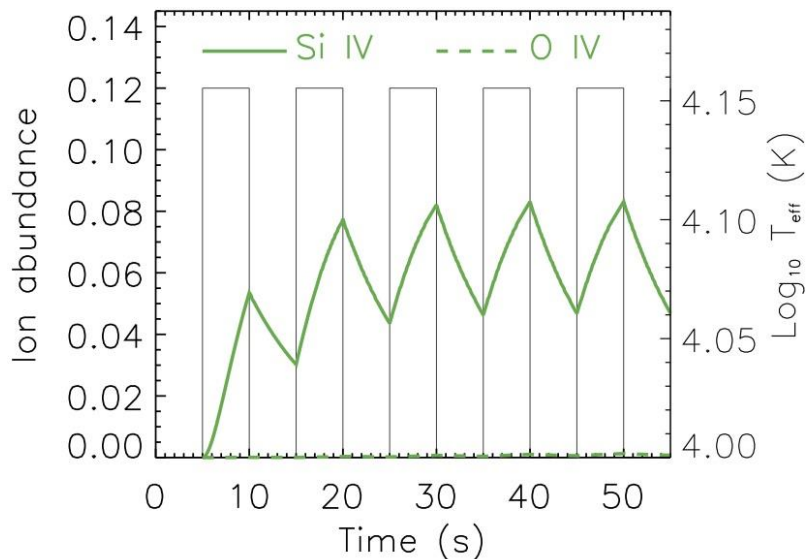
$P=10\text{s}$   $N_e=10^{10}\text{ cm}^{-3}$   $\kappa=3$



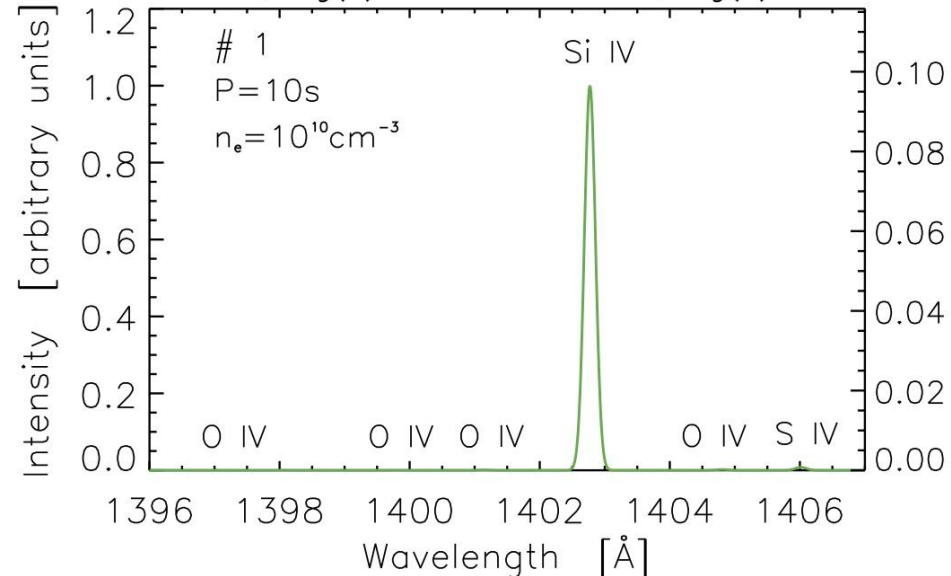
Maxwell,  $\text{log}(T)=4.00 \leftrightarrow \kappa=3, \text{log}(T)=4.30$



$P=10\text{s}$   $N_e=10^{10}\text{ cm}^{-3}$   $\kappa=5$

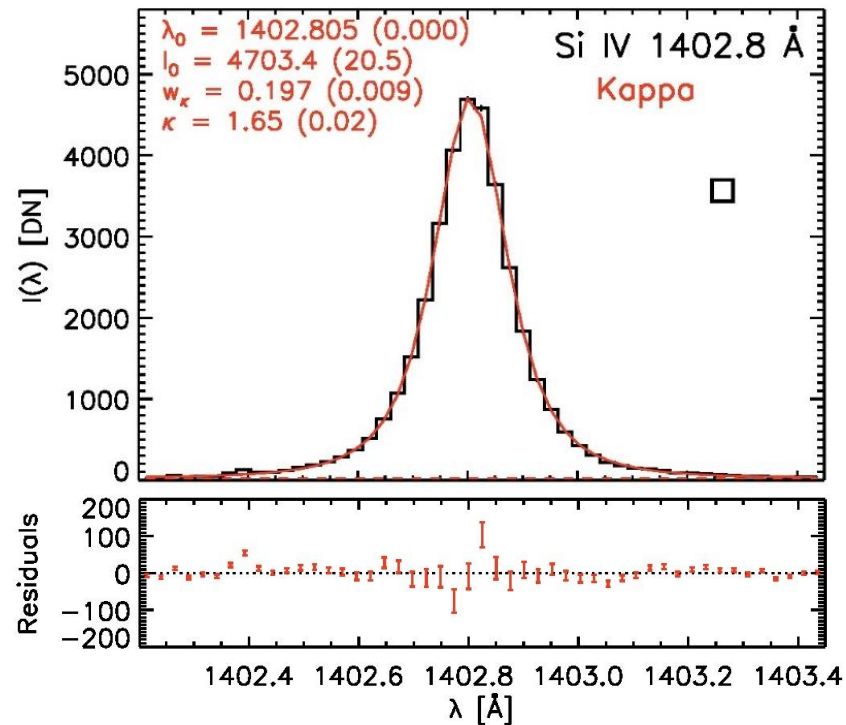


Maxwell,  $\text{log}(T)=4.00 \leftrightarrow \kappa=5, \text{log}(T)=4.15$



# Summary

- Detected non-Gaussian, highly symmetric profiles of TR lines in 120 pixels
- Typical  $\kappa$  values found from profiles are  $\kappa \approx 1.7 - 2.5$
- This is not an instrumental effect – we detected a Gaussian pixel
- Typical  $\kappa$  values found from fitting of relative intensities are  $\kappa \approx 2 - 3$  (but sensitive to abundances)
- The Si IV 1402.8 Å line is optically thin

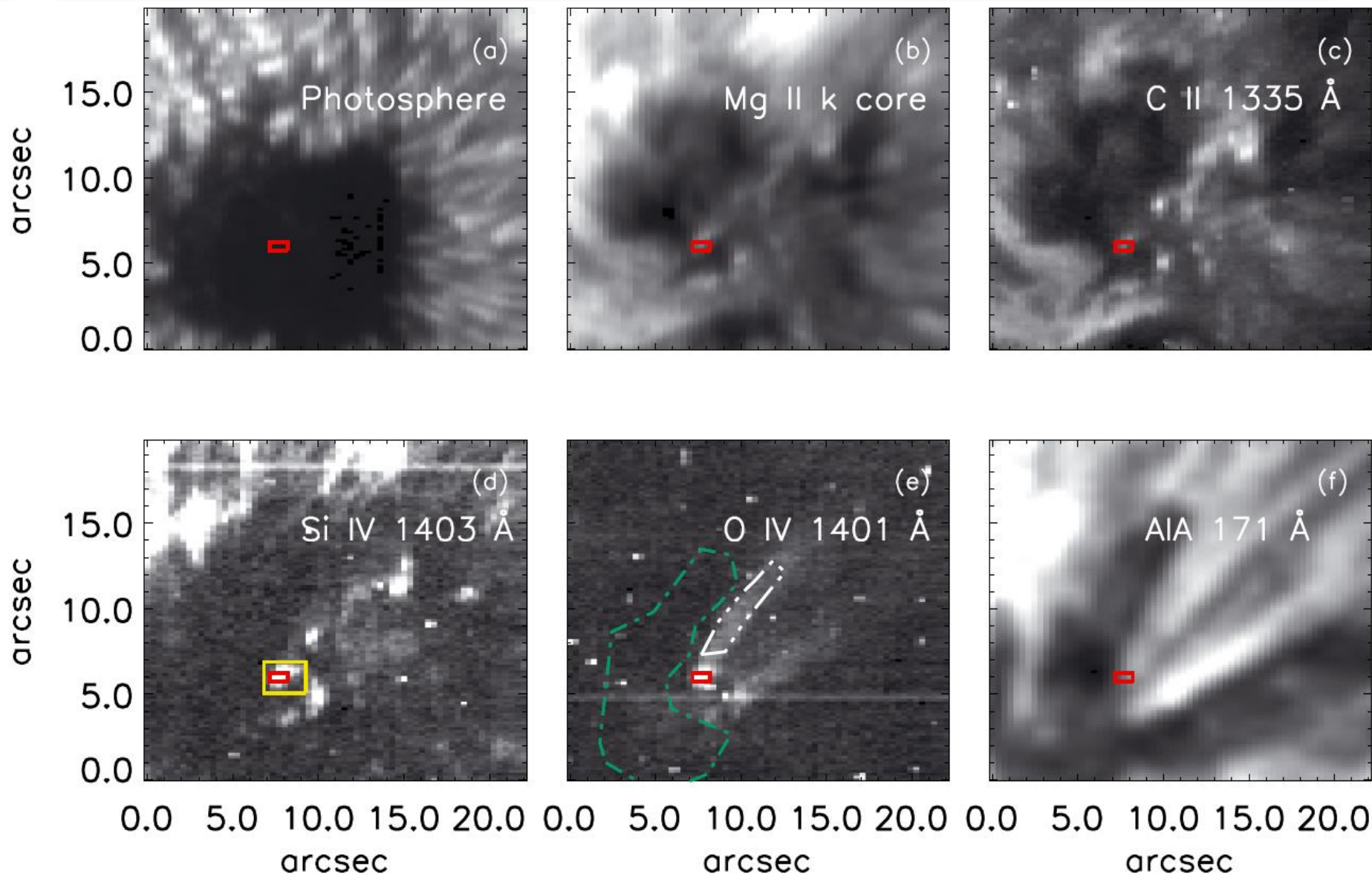


*Dudík et al. (2017), ApJ, 842, 19*

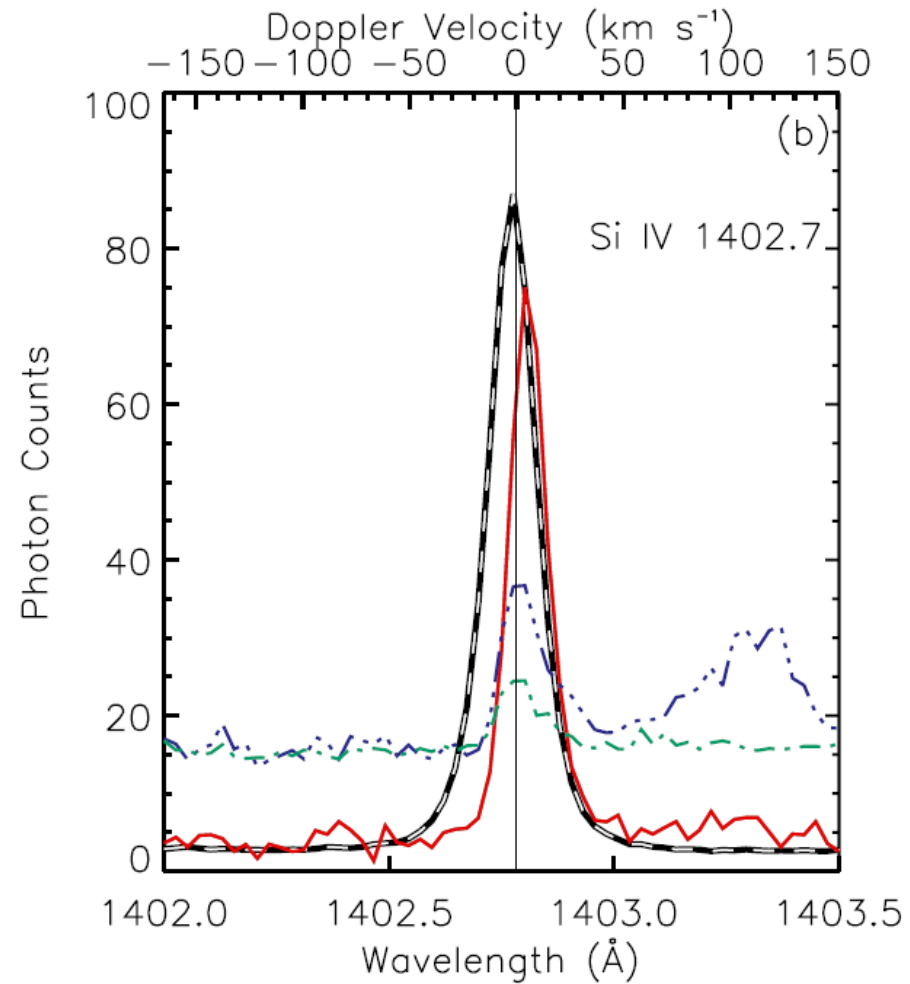
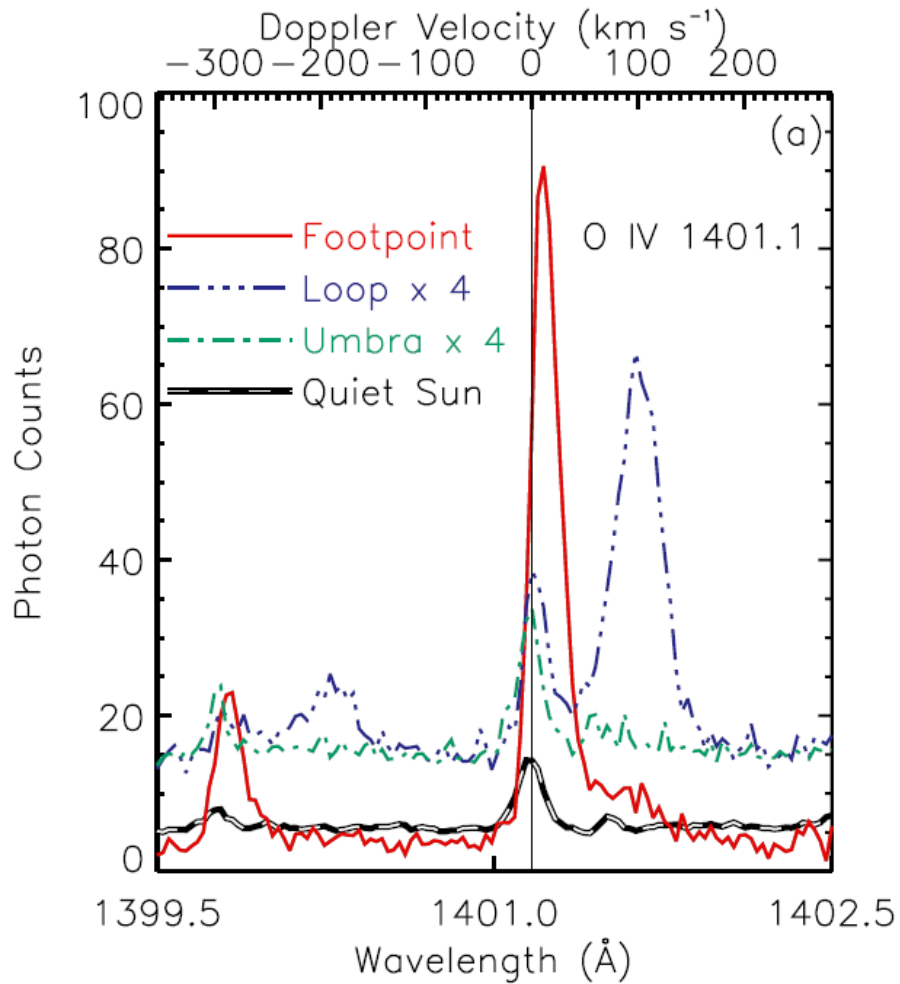
**Review on non-Maxwellians  
and non-equilibrium ionization:**

*Dudík et al. (2017),  
Solar Phys., accepted*

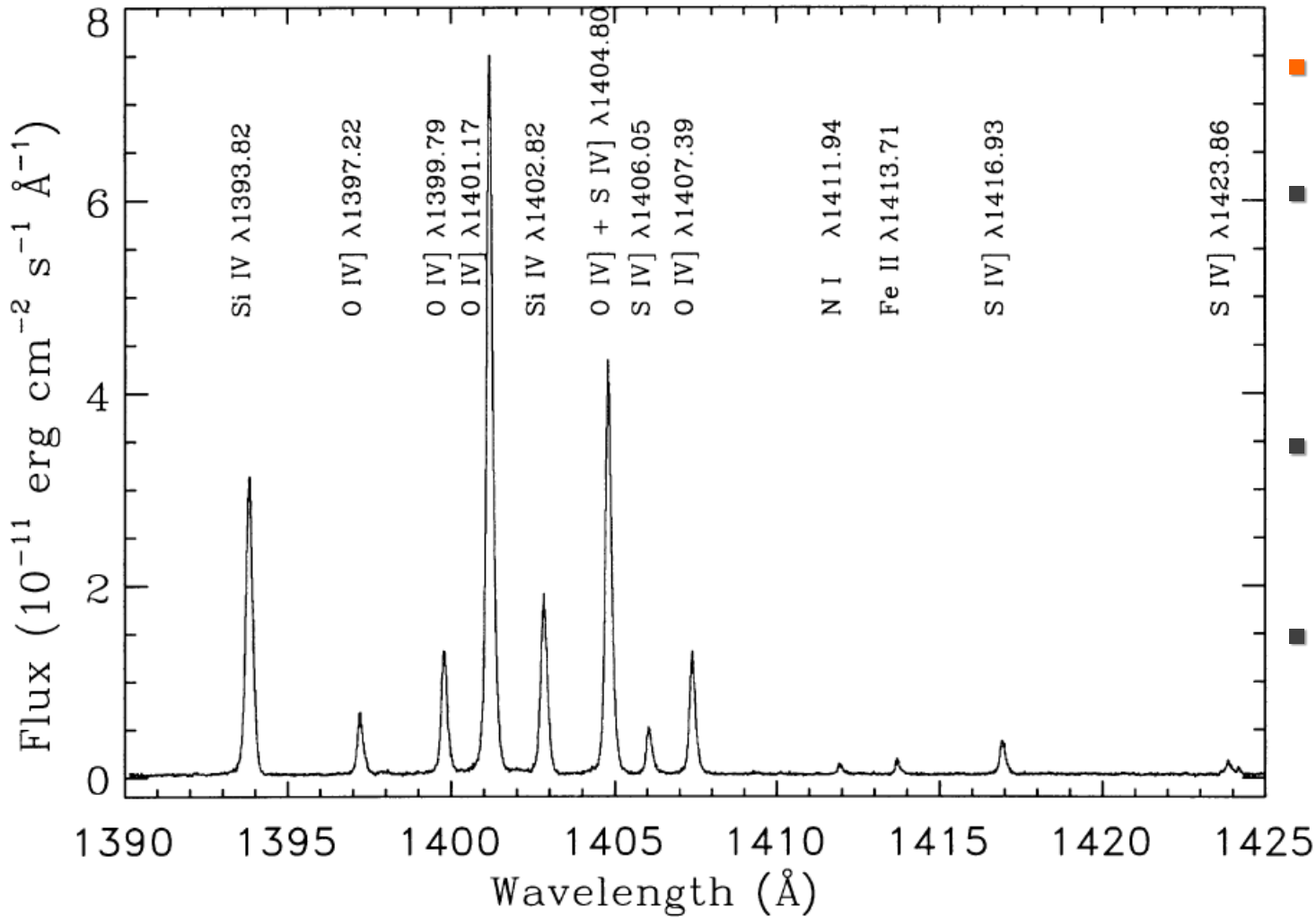
# O IV can be stronger than Si IV



# O IV can be stronger than Si IV



# Case of RR Telescopii Nebula



- **Symbiotic nova**
- **Mira-type giant and a white dwarf**
- **Last outburst in July 1948**
- **Observed by Hubble/GHRS**

*Harper et al. (1999), MNRAS, 303, L41*

*See also Keenan et al. (2002), MNRAS, 337, 901*

*Del Zanna et al. (2002), A&A, 385, 968*

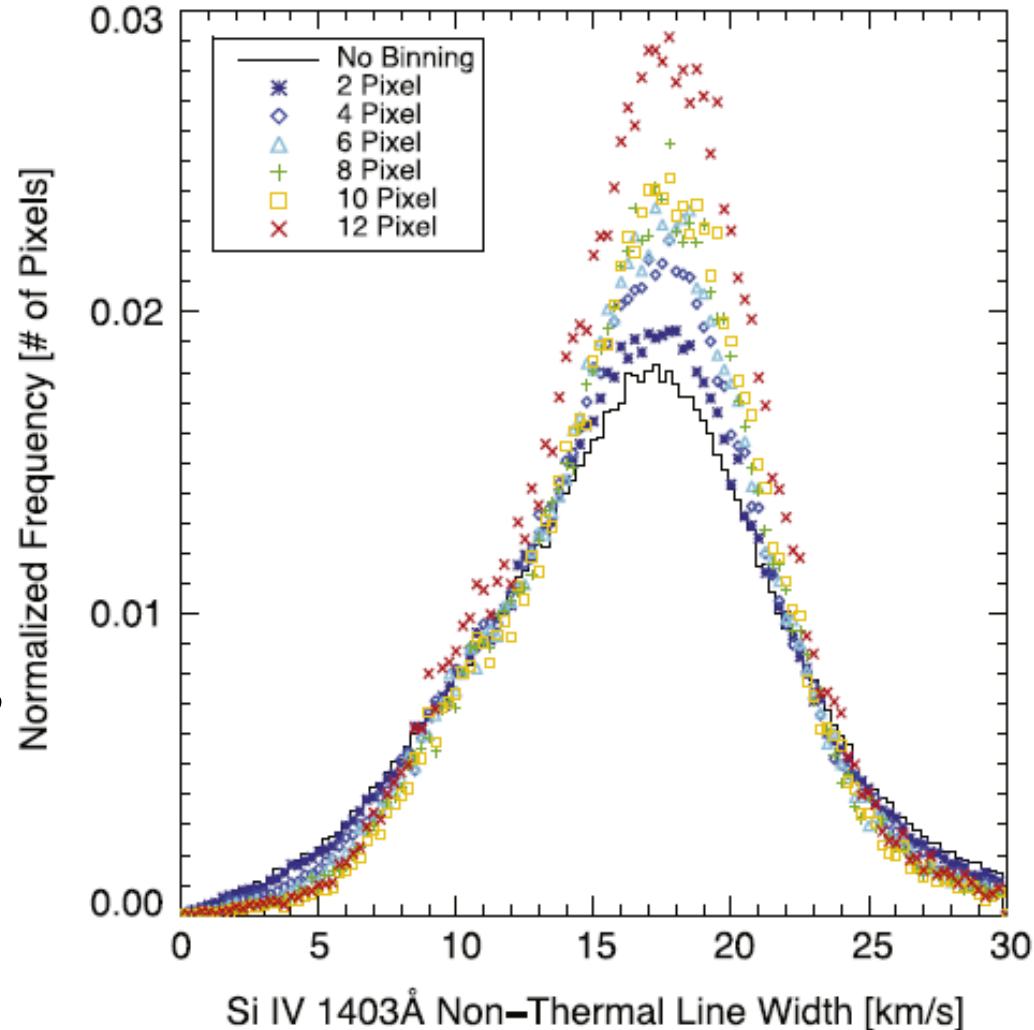
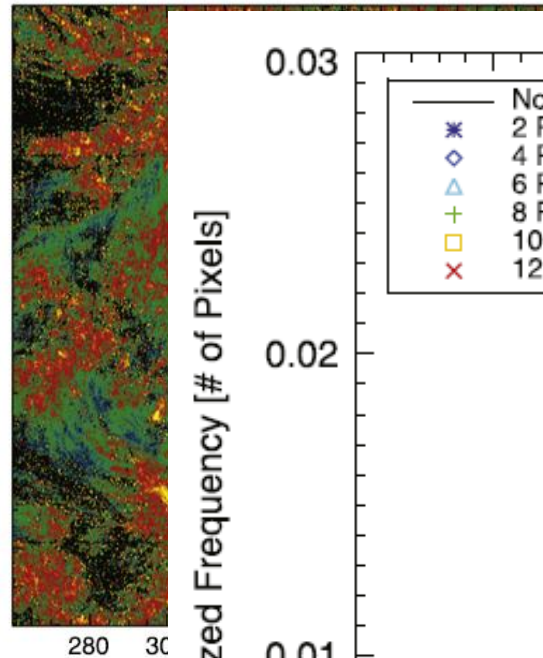
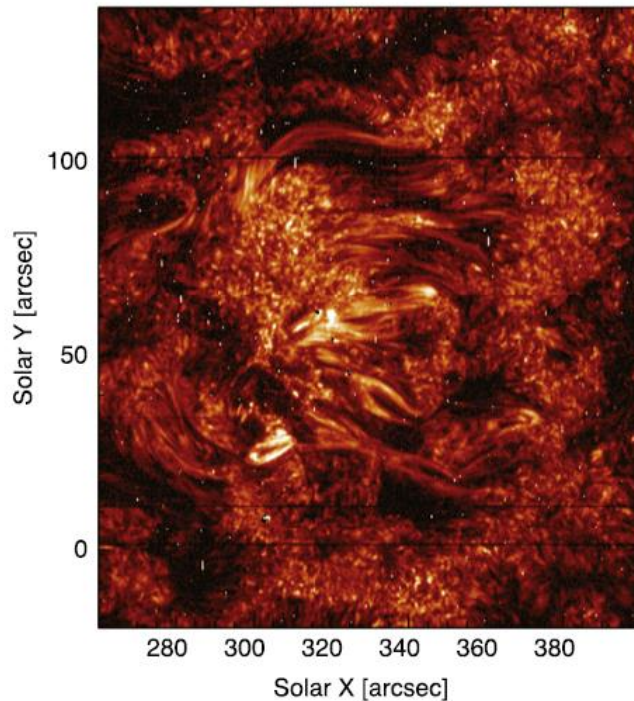
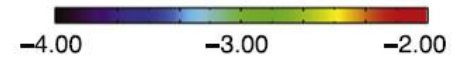
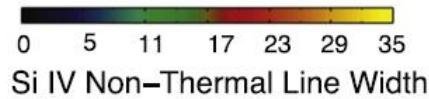


# Non-thermal widths

[log<sub>10</sub> DN/sec/px]



[km/s]



*De Pontieu et al. (2015), ApJ, 799, L12*

- Typical Si IV non-thermal widths are 15 – 20 km s<sup>-1</sup>
- Independent of spatial resolution

# Non-Equilibrium Ionization (NEI)

$$\frac{\partial Y_i}{\partial t} + \frac{\partial}{\partial s}(Y_i v) = n_e (I_{i-1} Y_{i-1} + R_i Y_{i+1} - I_i Y_i - R_{i-1} Y_i + \dots)$$

*e.g., Bradshaw & Mason (2003), A&A 401, 699*

where

$Y_i$  – population of ion  $+i$

$I_i$  – total ionization rate of ion  $+i$

$v$  – plasma velocity along  $s$  (loop)

$R_i$  – total recombination rate of ion

**If  $v = 0$ :**

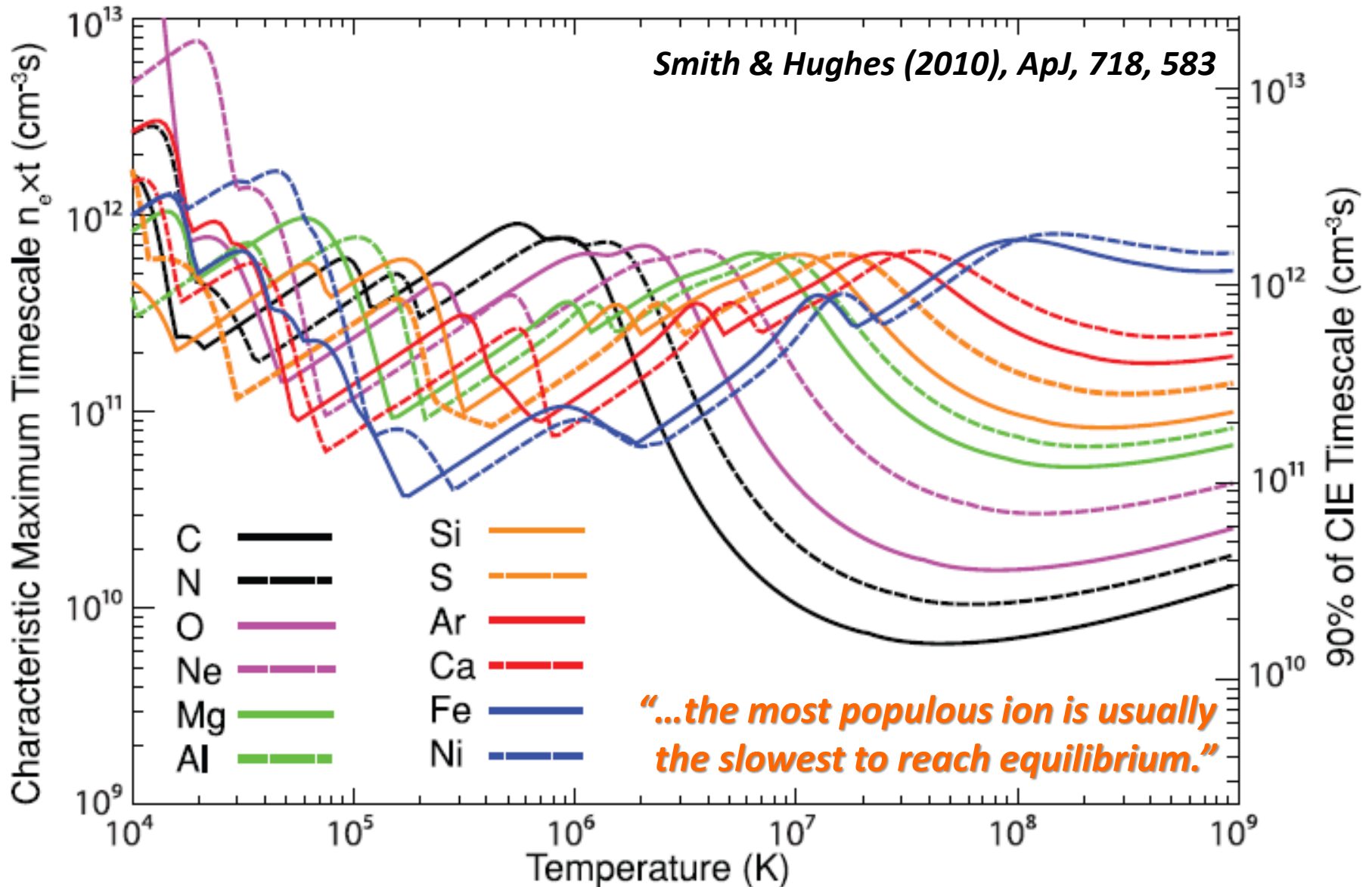
- Coupled set of  $Z+1$  first-order differential equations for  $Y_i$
- Can be re-cast as  $Z$  uncoupled first-order diff eqs using eigenvector basis
- Solution is a set of  $Z$  separate exponential functions
- Ionization equilibration timescale is given by the smallest eigenvalue  $\lambda_j$

$$Y_i(t, T_e) - Y_{i,\text{eq}}(T_e) = \sum_j W_{ji}(T_e) c_j \exp(-n_e \lambda_j t)$$

*Smith & Hughes (2010), ApJ, 718, 583*

*see also Golub et al. (1989), SoPh 122, 145; Reale & Orlando (2008), ApJ 684, 715*

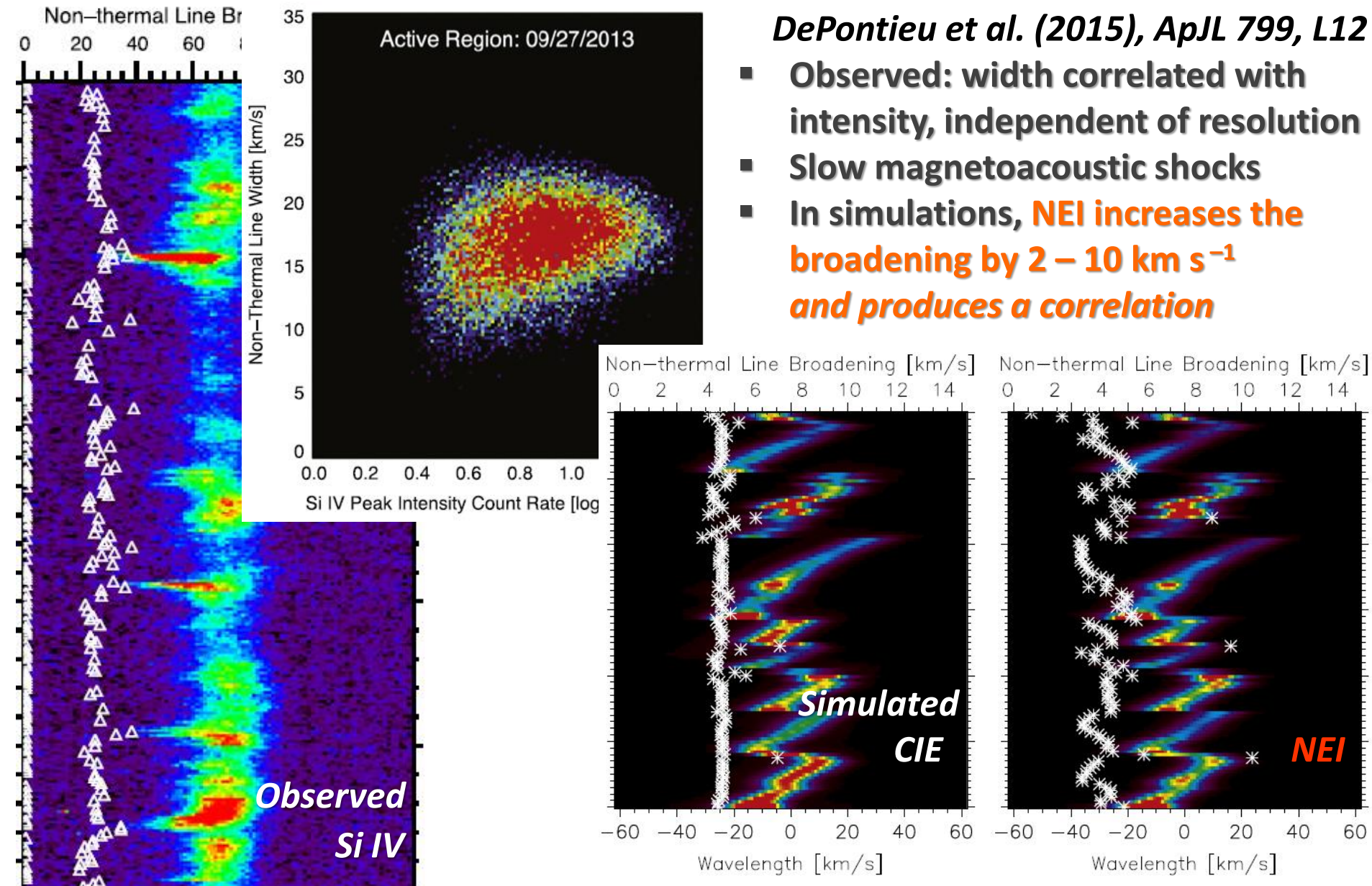
# NEI: Timescales



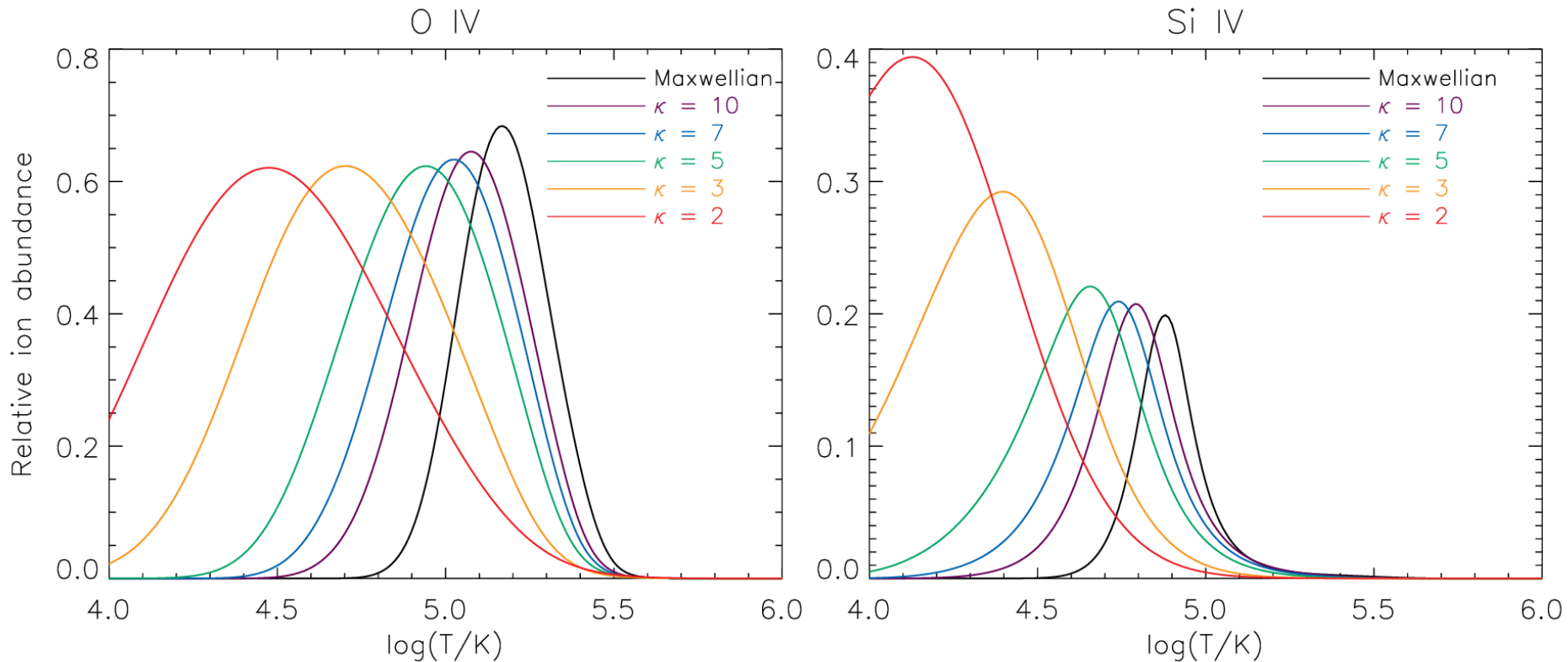
# NEI and non-thermal broadening

*DePontieu et al. (2015), ApJL 799, L12*

- Observed: width correlated with intensity, independent of resolution
- Slow magnetoacoustic shocks
- In simulations, **NEI increases the broadening by  $2 - 10 \text{ km s}^{-1}$  and produces a correlation**



# The $\kappa$ -distributions and TR lines

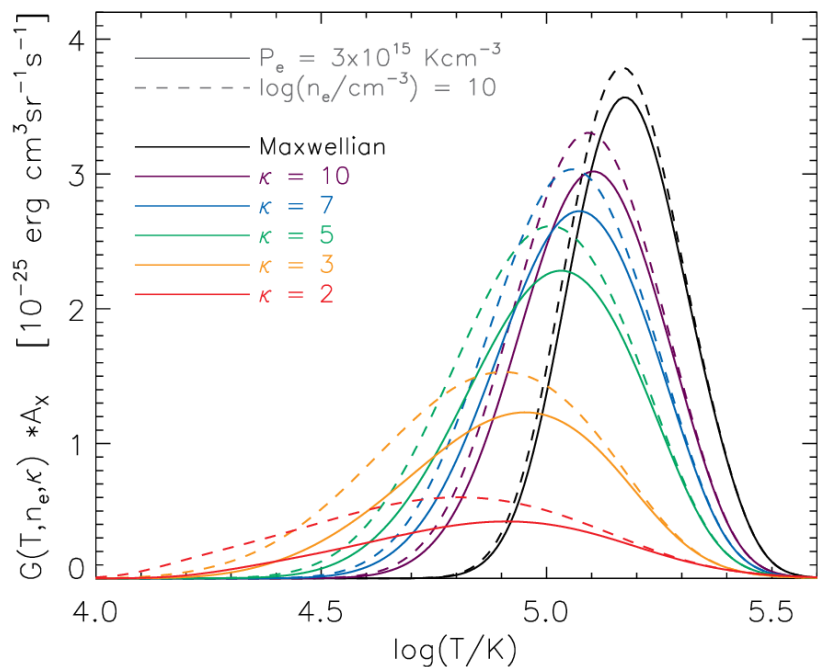


*Dzifčáková & Dudík (2013), ApJS, 206, 6*

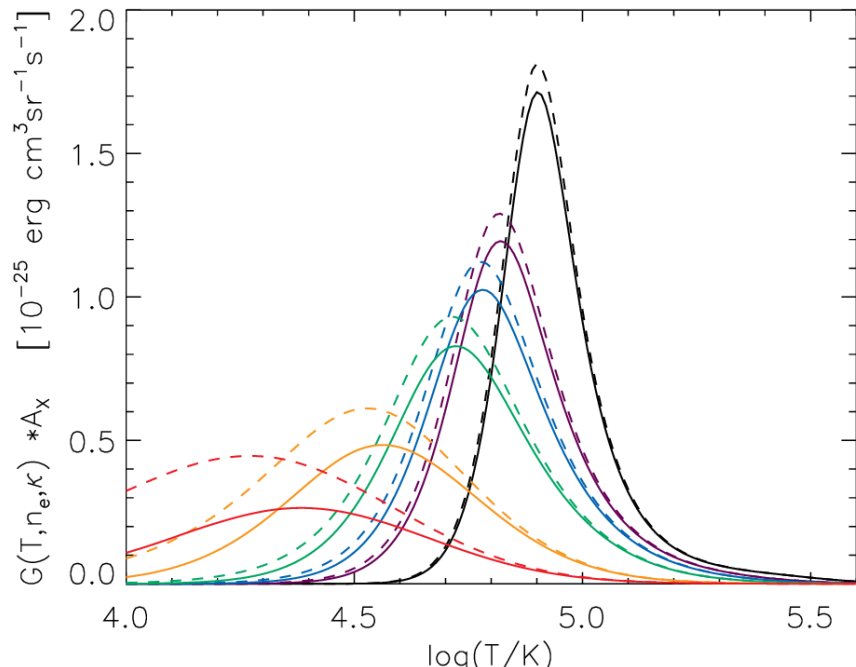
*Dudík et al. (2014), ApJL, 780, L12*

- **For TR lines, ion abundance peaks are shifted to lower  $T$**
- **Consequences of high-energy tail: strongly enhanced ionization**
- **Recombination not so strongly enhanced**

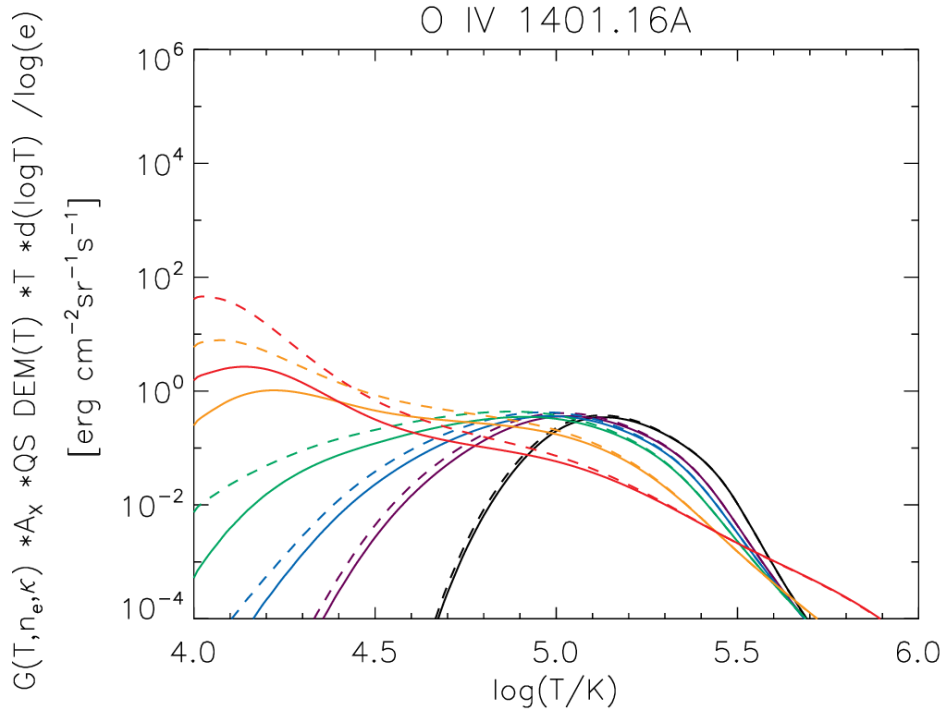
O IV 1401.16Å



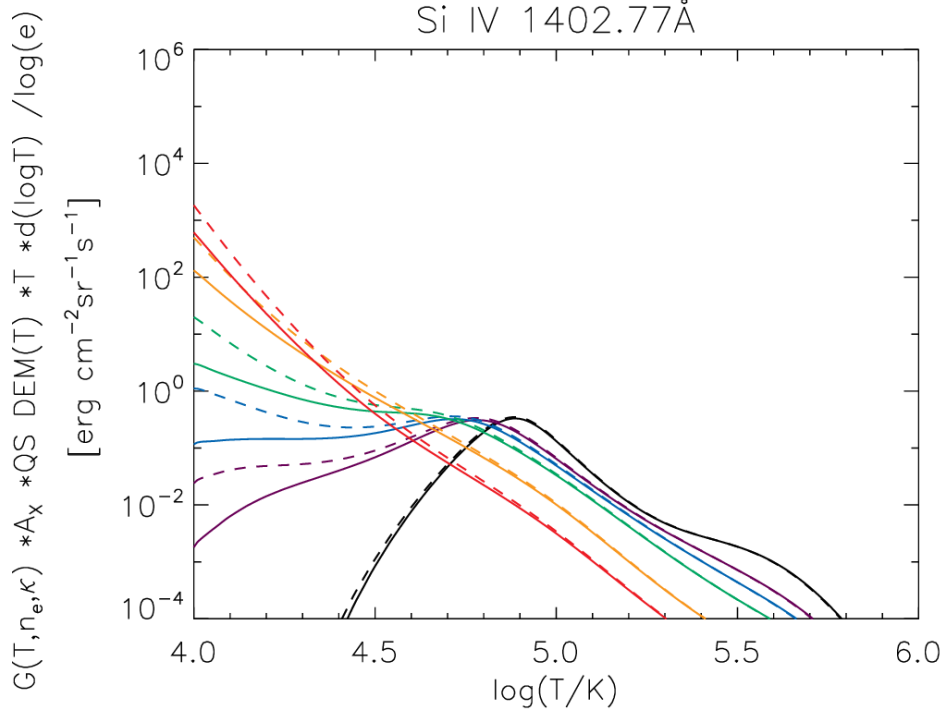
Si IV 1402.77Å



O IV 1401.16Å

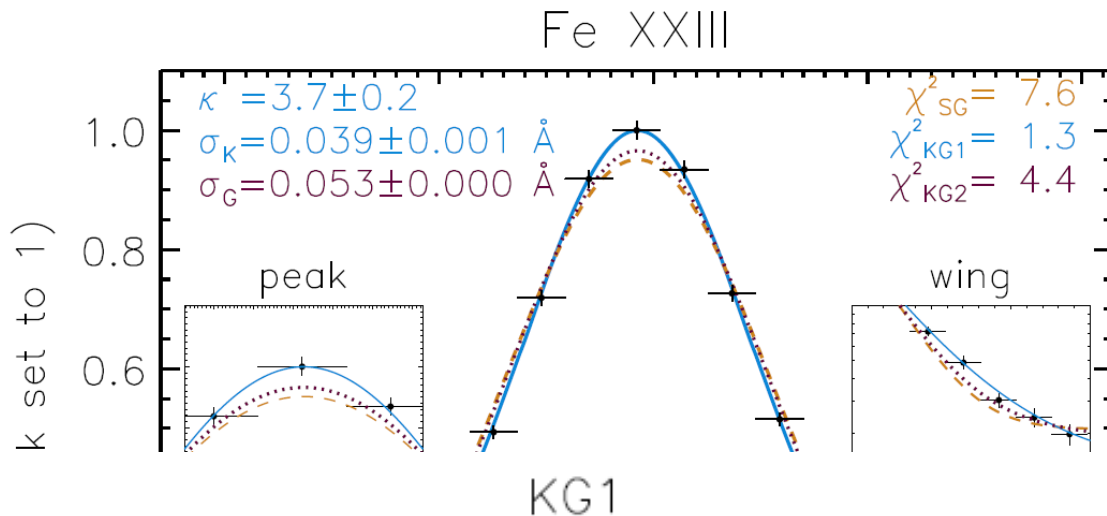


Si IV 1402.77Å





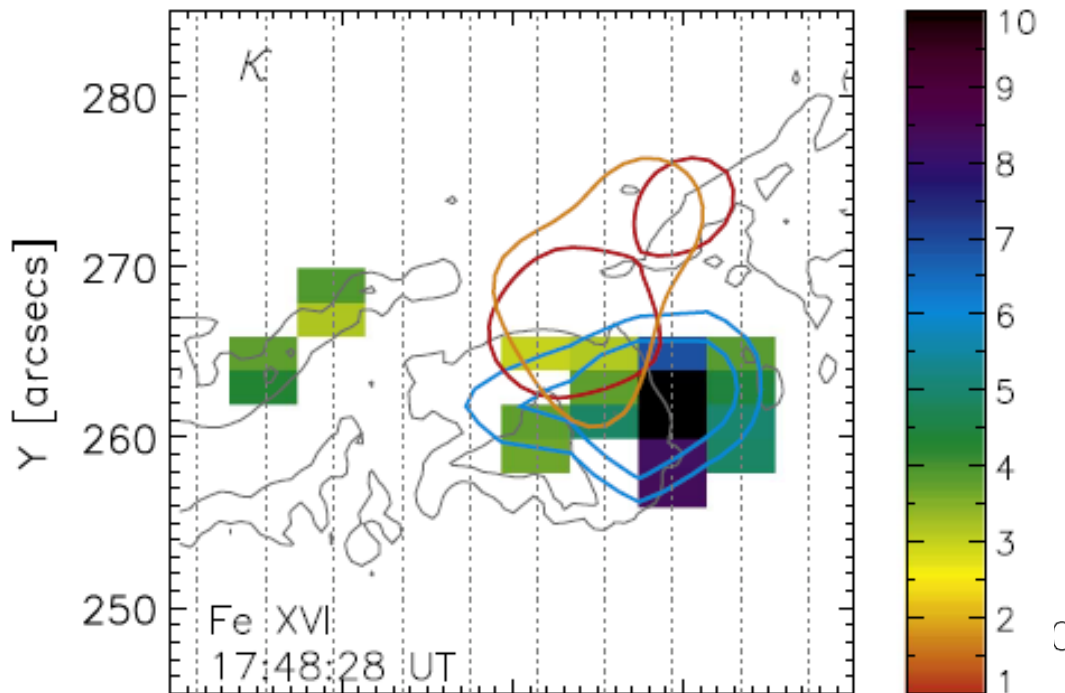
# The $\kappa$ -Profiles in *Hinode*/EIS



$$\begin{aligned}
 W(\lambda) &= G(\lambda) * K(\lambda) = A[0] + A[1] \\
 &\times \sum_{\lambda'} \exp\left(-\frac{(\lambda' - A[2])^2}{2\sigma_I^2}\right) \\
 &\times \left(1 + \frac{(\lambda - \lambda' - A[2])^2}{2A[3]^2 A[4]}\right)^{-A[4]+1},
 \end{aligned}$$

*Jeffrey et al. (2016),  
A&A, 590, A99*

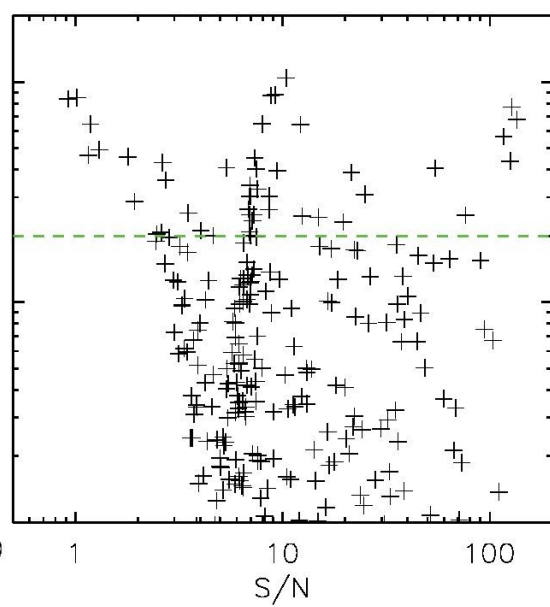
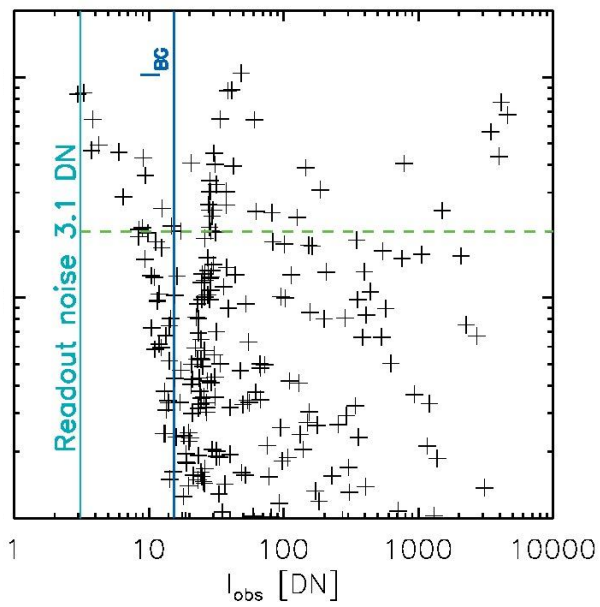
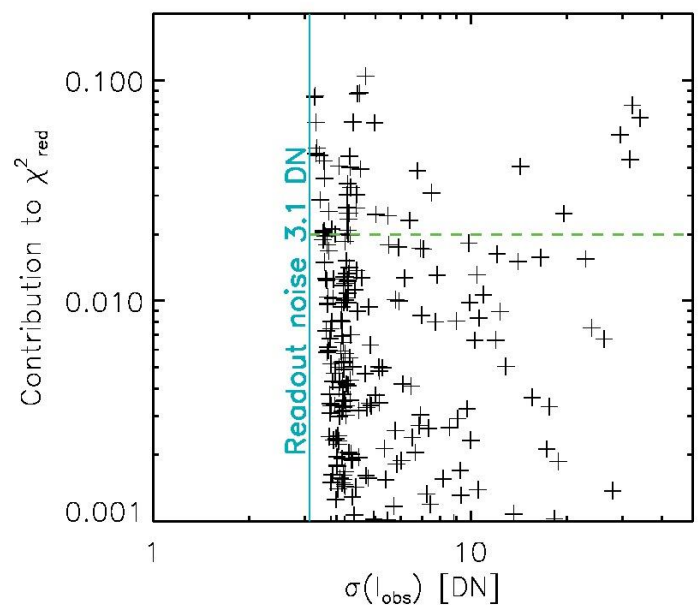
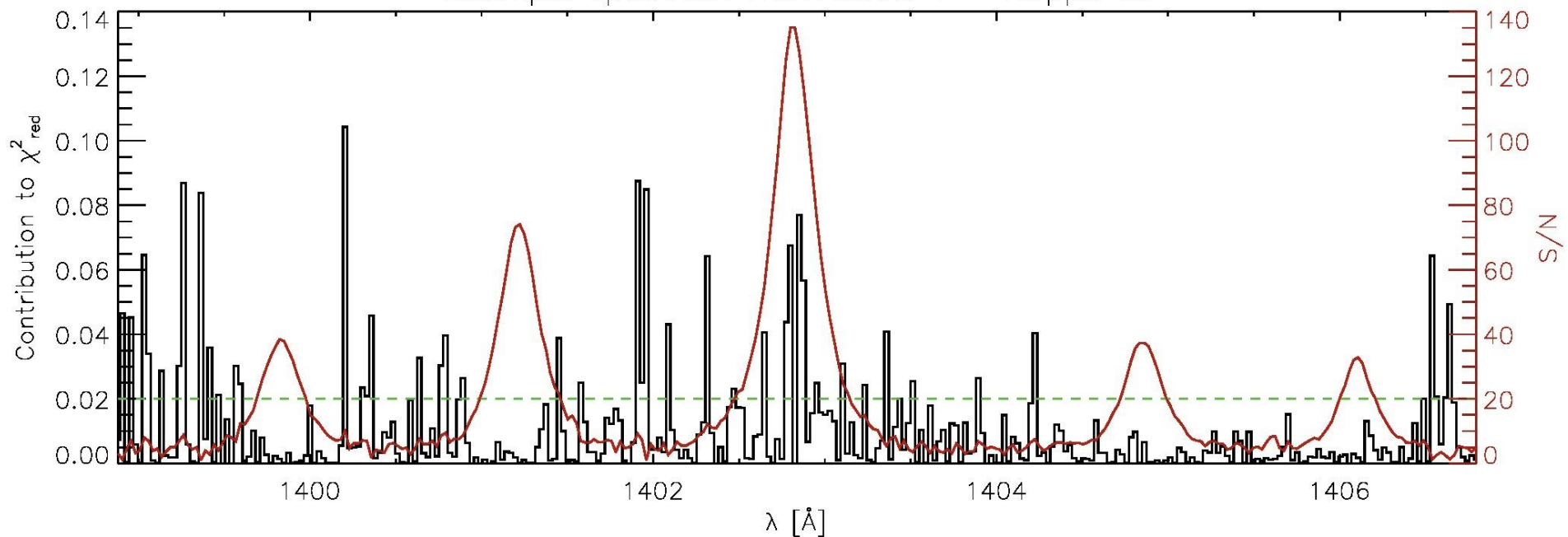
*Jeffrey et al. (2017),  
ApJ, 836, 35*



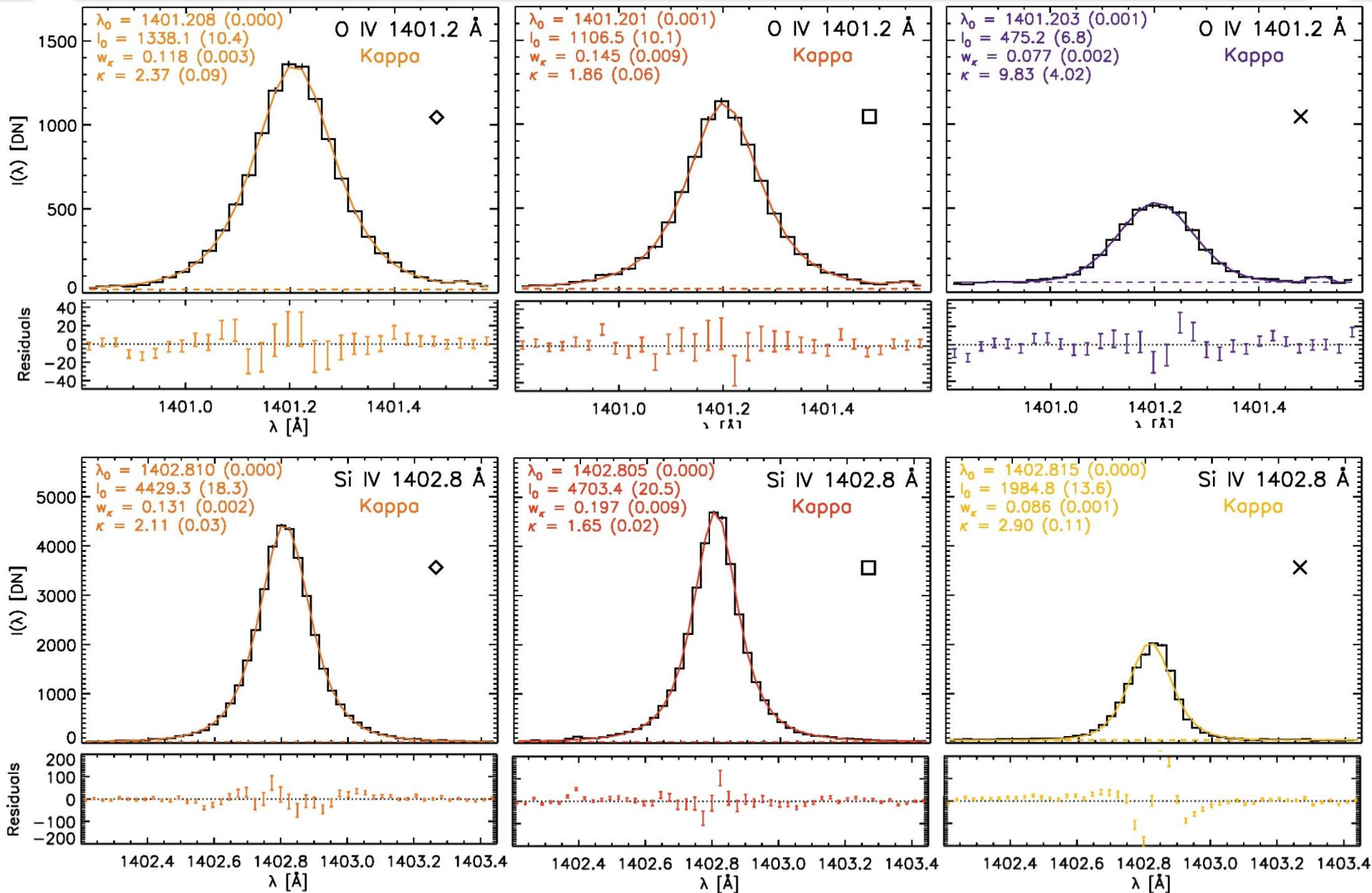
- Non-Maxwellian fitting of EIS flare lines
- Typically find  $\kappa \approx 2 - 3$
- Convolution with an instrumental profile, taken to be Gaussian



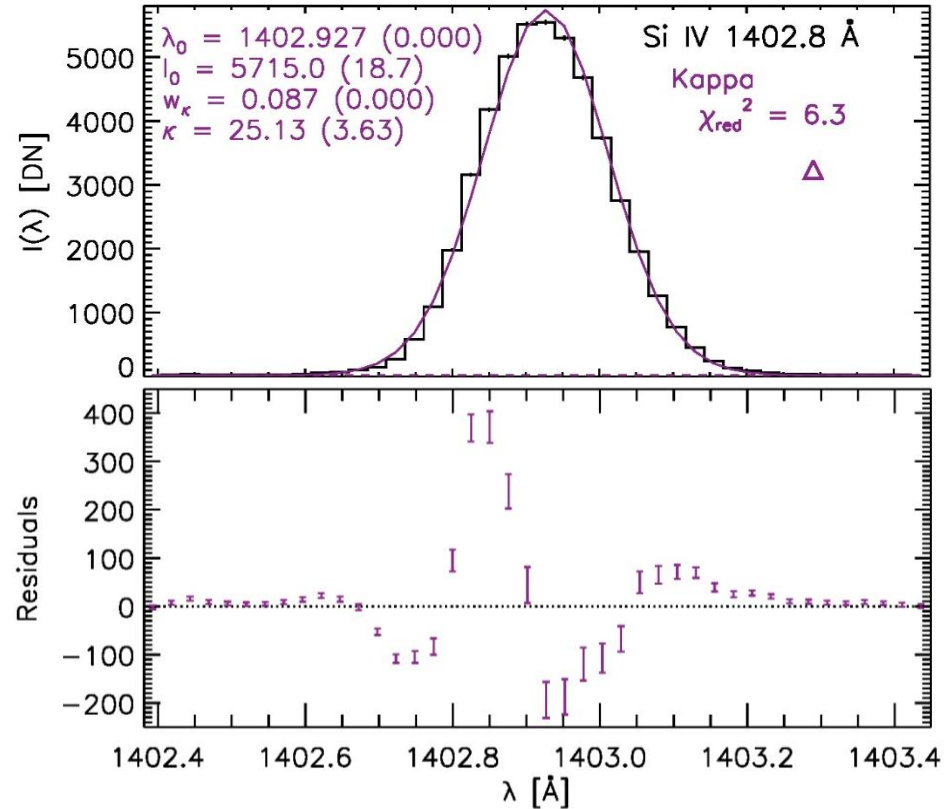
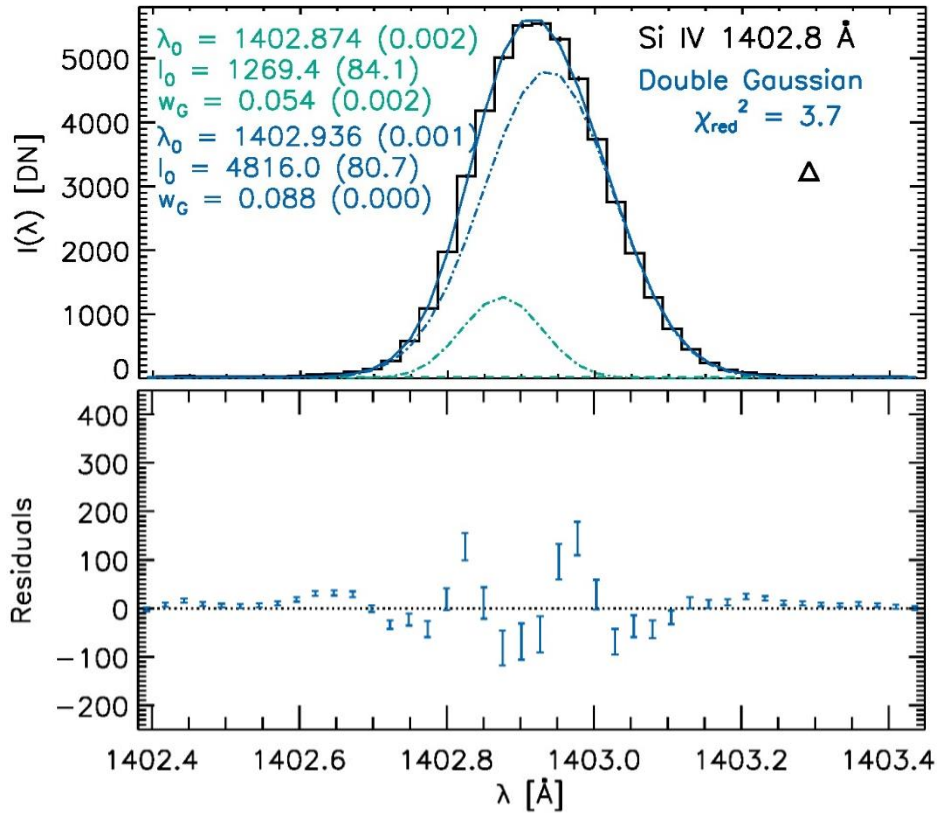
Example spectrum from Sect. 4 – Kappa fit



# Selected *IRIS* Spectra



# Multi-Component Si IV?



# Is the SI IV optically thick?

- The optical thickness is given by (e.g., Buchlin & Vial 2009, A&A, 503, 559):

$$\tau(\lambda) = \tau_0(\lambda_0)\Phi(\lambda) = \frac{\lambda_0^4 A_{ij} \Phi(\lambda)}{4\pi^{3/2} c \Delta \lambda_D} \frac{N(\text{Si}^{+3})}{N(\text{Si})} A(\text{Si}) \frac{N_{\text{H}}}{N_e} \langle N_e \rangle \Delta s$$

- For Maxwellian and *thermal* width, we get

$$\tau_0 \approx 0.26 f \frac{\langle N_e \rangle}{10^{10} \text{ cm}^{-3}}$$

- For  $\kappa = 2$ , the numerical factor is about 1.5  
(due to lower thermal width and higher  $N(\text{Si}^{+3}) / N(\text{Si})$ )

- For the *observed* width and a Maxwellian, we get

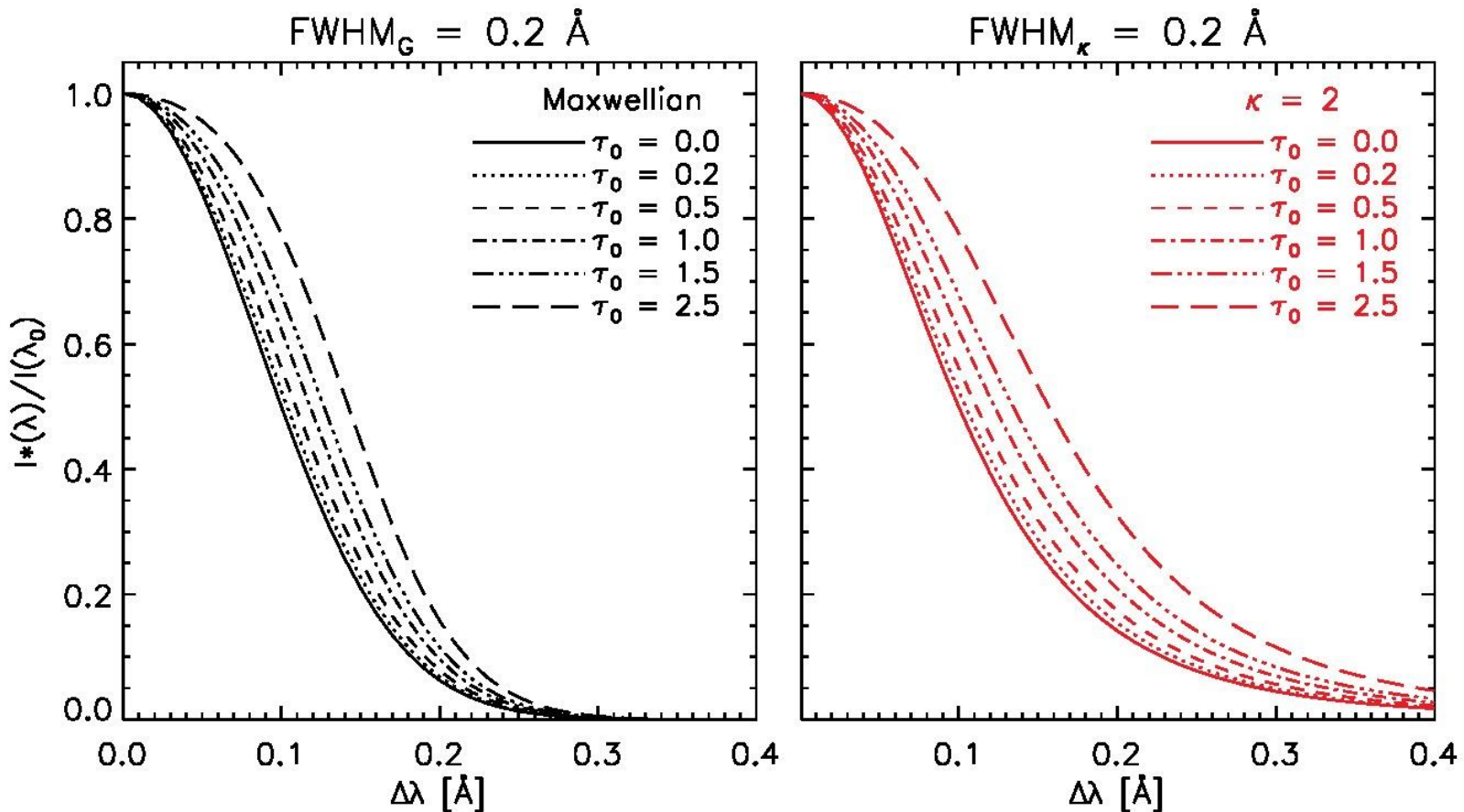
$$\tau_0 \approx 0.02 f \frac{\langle N_e \rangle}{10^{10} \text{ cm}^{-3}}$$

- For  $\kappa = 2$ , the numerical factor is about 0.06

# Is the SI IV optically thick?

- If the line is optically thick, then the profile should be (for  $S = \text{const.}$ )

$$I^*(\lambda) = \int_0^{\tau(\lambda)} S_\lambda \exp(-t_\lambda) dt_\lambda = S_\lambda [1 - \exp(-\tau(\lambda))]$$



# Multi-Component Si IV?

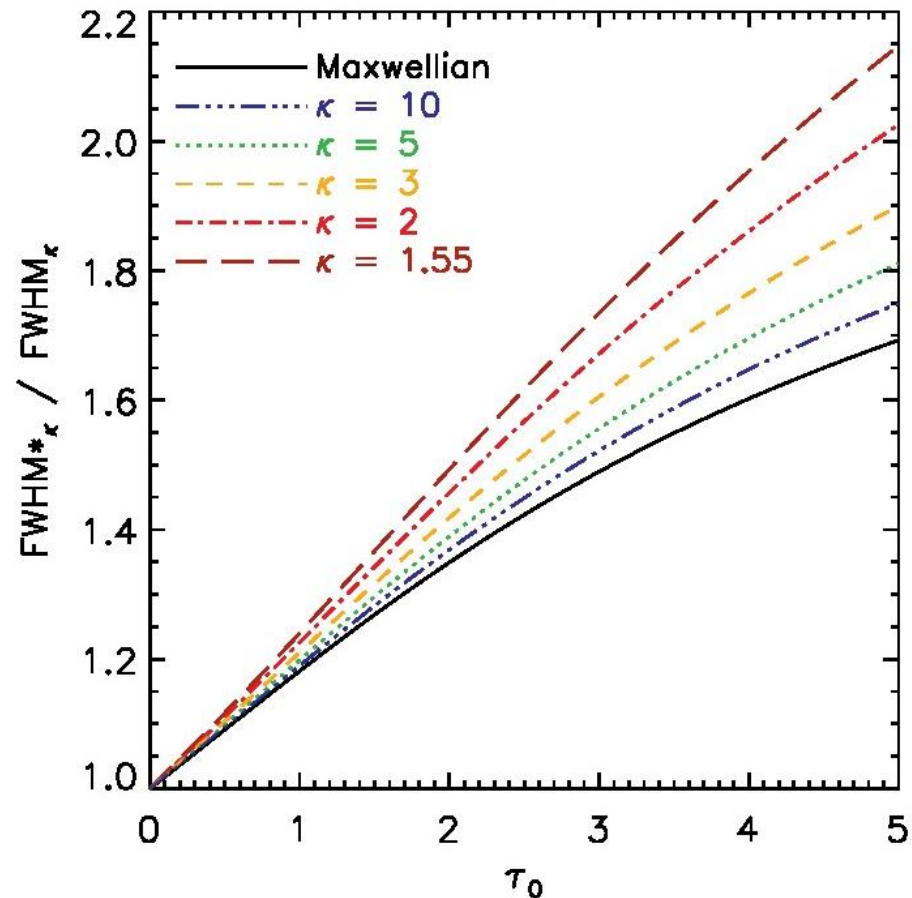
- The FWHM changes as

$$\text{FWHM}_{\kappa}^*(\tau_0)^2 = 8(\kappa - 3/2)w_{\kappa}^2 \left[ \left( \frac{\tau_0}{\ln(2) - \ln(\exp(-\tau_0) + 1)} \right)^{\frac{1}{\kappa}} - 1 \right]$$

- Recall that the FWHM of the Si IV line is the same as for the O IV and S IV

- For solar conditions, O IV lines are always optically thin because of their small  $A_{ij}$

- $\Rightarrow$  the Si IV is optically *thin*



# Contents

- I. **Transition-Region Lines: Challenges**
  - Allowed-to-intercombination ratios
  - Redshifts and line widths
  - Non-Gaussian line profiles
  
- II. ***Interface Region Imaging Spectrograph (IRIS) TR Observations***
  - Symmetric line profiles
  - Fitting with double Gaussians and a  $\kappa$ -distributions
  - Distribution of non-Gaussian profiles
  
- III. **Line Intensity Analysis**
  - Consistent  $\kappa$ -distributions?
  
- IV. **Leftovers**
  - Is the Si IV line optically thick?